DEVELOPMENT OF A POLY ANILINE BORONIC ACID (PABA) CARBON DIOXIDE (CO_2) SENSOR FOR USE IN THE AGRI-FOOD INDUSTRY

A Thesis

submitted to the Faculty of Graduate Studies

The University of Manitoba

in partial fulfillment of the requirements for the degree of

Doctor of Philosophy

by

Sureshraja Neethirajan

Department of Biosystems Engineering

University of Manitoba

Winnipeg, Canada

R3T 5V6

UNIVERSITY OF MANITOBA
FACULTY OF GRADUATE STUDIES
FINAL ORAL EXAMINATION OF THE PHD THESIS

The undersigned certify that they have read, and recommend to the Faculty of Graduate Studies for acceptance, a PhD thesis entitled:

Development of A Carbon Dioxide (CO_2) Sensor For Agri-Food Industry Poly Aniline Boronic Acid (PABA) USE in the

by

Sureshraja Neethirajan

In Partial fulfilment of the requirements for the degree: Doctor of Philosophy

[redacted]
Dr. Digvir Jayas, Advisor

[redacted]
Dr. Michael Freund

[redacted]
Dr. Cyrus Shafai

[redacted]
Dr. Noel D.G. White

[redacted]
External Examiner
Dr. G.S. Vijaya Raghavan
Agriculture & Biosystems Engineering

Date of Oral Examination: Wednesday, September 2, 2009

The Student has satisfactorily completed and passed the PhD Oral Examination.

[redacted]
Dr. Digvir Jayas, Advisor

[redacted]
Dr. Michael Freund

[redacted]
Dr. Cyrus Shafai

[redacted]
Dr. Noel D.G. White

[redacted]
Dr. James D. House, Chair of PhD Oral

Dr. G.S. Vijaya Raghavan

(nb. The signature of the Chair does not necessarily signify that the Chair has read the thesis.)

THE UNIVERSITY OF MANITOBA

FACULTY OF GRADUATE STUDIES

****

COPYRIGHT PERMISSION

DEVELOPMENT OF A POLY ANILINE BORONIC ACID (PABA) CARBON DIOXIDE (CO_2) SENSOR FOR USE IN THE AGRI-FOOD INDUSTRY

A Thesis/Practicum submitted to the Faculty of Graduate Studies of The University of Manitoba in partial fulfillment of the requirement of the degree

of

Doctor of Philosophy

by

Sureshraja Neethirajan

ABSTRACT

In the agri-food industry, carbon dioxide sensors can be used for process control, monitoring quality, and assessing safety. A carbon dioxide sensor was developed using poly aniline boronic acid (PABA) conducting polymer as the electrically conductive region of the sensor for use in the agri-food industry and was demonstrated for use in detecting incipient or ongoing spoilage in stored grain. The developed sensor dynamically detected up to 2455 ppm CO_2 concentration levels. The performance of the sensor in measurements of low concentrations of dissolved CO_2 was characterized using standard solutions of $NAHCO_3$. The dynamic range for the detection of H_2CO_3 was $4.91X10^{-4}$ to 9.81X10-3 mol L^{-1}. The dc resistance values decreased with increasing CO_2 concentration indicating an increase of conductivity due to increase in the amount of protonation.

The developed CO_2 sensor was evaluated for the influence of temperature (by storing it at – 20°C and 0°C as well as at operating temperatures of +10°C to 55°C) and relative humidity (from 20 to 70%). Temperature dependence of sensor's resistance values were observed possibly due to the change in conduction mechanism at different temperatures. The variation in the resistance with humidity was curvi-linear and repeatable, indicating that humidity has a less pronounced effect on the sensor's performance. The sensor's response to changes in CO_2 concentrations at various humidity and temperature levels was stable indicating that the sensor can detect CO_2 levels under fluctuating environmental conditions. The response of the PABA film to CO_2 concentration was not affected by the presence of alcohols and ketones, proving that the developed CO_2 sensor is not cross-sensitive to these compounds which may be present in spoiling grain. The sensor packaging components were selected and built in such a way to avoid contamination of the sensing material and the substrate by undesirable

components including grain dust and chaff. The developed conducting polymer CO_2 sensor exhibited dynamic performance in its response, recovery times, sensitivity, selectivity, stability and response slope when exposed to various CO_2 levels inside simulated grain bulk conditions.

ACKNOWLEDGMENTS

“ Some men see things as they are and say “why”;

I dream of things that never were and say “why not.” “

- *George Bernard Shaw*

There are many people who helped me to finish this thesis by giving moral encouragement, professional advice, and by providing technical help to perform experiments.

I sincerely thank my advisor, Dr. Digvir Jayas (Department of Biosystems Engineering) for his guidance, stimulating suggestions, mentorship and encouragement. His company, positive attitude, wisdom, words of comfort and fatherly treatment will be remembered lifelong.

My sincere thanks are due to Dr. Noel White (Agriculture and Agri-Food Canada) and Dr. Michael Freund (Department of Chemistry) for the valuable discussions that I had with them during the course of this research.

Many thanks to Dr. Cyrus Shafai and Dr. Douglas Thomson (Department of Electrical and Computer Engineering) for reviewing my research work and for contributing their expertise to the grain quality sensor development team.

The cooperation I received from other faculty members of the Department of Biosystems Engineering (University of Manitoba) is gratefully acknowledged. A sincere thank you is passed to the technicians (Matt McDonald, Dale Bourns, Robert Lavallee – Biosystems Engineering; Wayne Buchannon – Chemistry; and Colin Demianyk –

Agriculture and Agri-Food Canada) and the administrative staff (Debby Watson, Evelyn Fehr and Derek Inglis) of the Department of Biosystems Engineering for their kind help.

The Canada Research Chairs (CRC) program and the Natural Sciences and Engineering Research Council (NSERC) of Canada are gratefully acknowledged for funding this project. My gratitude extends to the Canadian Wheat Board (CWB) for the CWB Graduate Fellowship; NSERC for the Canada Graduate Scholarship, NSERC Nano Innovation Platform Award, and NSERC Summer Internship award; Japan Society for the Promotion of Science (JSPS) for the JSPS fellowship; the University of Manitoba for the Muir Award for Academic Excellence, Graduate Fellowship and Edward Toporeck Graduate Fellowship, and UMSU and GSA scholarships.

I also want to thank my parents, who taught me the value of hard work by their own example. I would like to share this moment of happiness with my brother and sister who rendered me enormous support during the whole tenure of my research. Finally, I would like to thank all whose direct and indirect support helped me in completing my thesis in time.

Vision

" Looking up gives light, although at first it makes you dizzy "

- Rumi

Dedicated to my beloved guru, *Sadhguru Jaggi Vasudev*

Table of Contents

LIST OF TABLES

LIST OF FIGURES

1. INTRODUCTION

The evolving agriculture and food system has entered into a consumer driven era with consumers demanding food safety, quality and convenience. To analyze, design, develop, manage, control and characterize the biological and environmental processes in the agri-food industry, there is a need to collect data. This has necessitated the agri-food industry to increasingly rely on sensor technology. For example, sensors are used in the field for monitoring of environmental parameters to help producers in conducting more efficient irrigation or pest control programs, on harvesting machinery for measuring yield per unit area, during storage for measurement of product temperature, for post harvest grading and sorting of fruits and vegetables, and for online monitoring of process parameters during processing. Hence, data collecting sensors are essential for real-time decision-making.

Sensors for the agri-food industry exhibit several differences compared to the traditional industrial sensors in terms of the measurement parameters as well as the environment. The users of agricultural sensors require inter-operable measurement framework and relative ease in the interpretation of sensor data. The agri-food processes are inherently more variable due to their biological nature (Neethirajan et al., 2009) thus sensors require the capability to handle this variability. The environment surrounding the raw as well as the processed agricultural materials is usually complex. Presence of multiple microorganisms

and other biological agents further makes the sensing of parameters in the agri-food industry very challenging.

Plant gas exchange, atmospheric gas monitoring, soil carbon dioxide (CO_2) flux, biogas composition monitoring (Rego and Mendes, 2004; Reich, 1945) are areas in which monitoring CO_2 becomes essential. Monitoring of CO_2 with the help of sensors is critical for freeze damage detection in oranges (Tan et al., 2005); for processing of alcohols and beverages (Marazuela et al., 1998), and for methanol and urea production.

Food packaging is often done under a modified atmosphere of nitrogen (N_2), CO_2, and oxygen (O_2), specific to a product and with a purpose to prevent microbial spoilage. Carbon dioxide is widely used in modified-atmosphere packaging and a decrease in its concentration is a sign of leakage in a package. Freshness and safety of modified atmosphere food packages can be determined by detection of CO_2 concentrations (Smolander et al., 1997; Jones, 1923). High CO_2 levels can affect quality of French fries during processing and therefore, monitoring of CO_2 levels can be used for controlling ventilation in potato storage facilities (Jayas et al., 2001).

1.1 Sensors for Grain Storage

The world annual grain production is about 2 Gt (billion metric tonnes) (USDA, 2007). The grains and oilseeds sector is a major component of the Canadian

agriculture industry, with exports valued at over $10 billion annually (Statistics Canada, 2007).

Stored grain bulks are ecological systems where communities of insects, mites and microflora interact with abiotic variables to cause spoilage (Wallace and Sinha, 1981). While the importance of proper grain storage has been realized, post-harvest losses continue to range from 9% in North America to 50% in developing countries (FAO, 2000). Any loss in quality or quantity of the produced grain has far-reaching economic effects.

During the spoilage of grain, CO_2, moisture and heat are produced by the metabolism of the grain, fungi, insects and mites, and distinct odours are released. Evolution of excessive CO_2 from a grain mass is an indicator of deteriorating grain. Increased levels of CO_2 indicate that insects, mould, or excessive respiration are present. Carbon dioxide and odour volatiles from biological pests increase during spoilage and can be used as a reliable indicator of incipient grain spoilage (Jayas 1995; Magan and Evans, 2000; Maier et al., 2006).

Grain odours are caused by complex mixtures of compounds having various degrees of volatility. Volatiles can come from the grain itself, fungi, mites or insects. Although numerous insect and fungal species can occur within a grain bulk, *Aspergillus* and *Penicillium* genera of moulds, rusty grain beetle (*Cryptolestes ferrugineus* (Stephens)) and red flour beetle (*Tribolium castaneum* (Herbst)) are the common species in Canadian grain (White, 1995). Fungi can

produce a series of alcohols (3-methyl-l-butanol, 1-octen-3-ol, 1-octanol and 3-octanone) in bulk wheat (Sinha et al., 1988). The rusty grain beetle produces a mixture of 4, 8-dimethyl-E, 4,8-decadienolide and ferrulactone II in grain bins (Loschiavo et al., 1986). Flour beetles (*Tribolium* species) produce functionalized aromatics, e.g.,1,4-dimethoxybenzene, 2-methyl-1, 4-dimethoxybenzene, and 2-ethyl-1,4-dimethoxybenzene (Seitz and Ram, 2000).

Until now, researchers have measured volatile compounds from individual sources such as insects or moulds within the grain bulk. A survey conducted by Madrid et al. (1990) showed that co-occurrence of insect species, molds and mites caused spoilage in Canadian grain bins. Hence, there is a need to identify volatile compounds evolving from grains, in particular with the presence of multiple species. For the fabrication of odour sensor arrays as an early warning grain quality monitoring system, the identification of volatile metabolites in stored-grain head space from multiple species is essential.

Instruments capable of sensing CO_2 concentrations of 0.1% (atmospheric levels are 0.038%) will detect spoilage during stored grain in 80% of deteriorating bulks in farm granaries (Singh et al., 1983; Muir et al., 1985). Detection and measurement of extreme levels of CO_2 atmospheres by suitable sensors can protect the safety and health of farmers in confined spaces such as manure storage facilities and grain silos (USDA, 1996).

Ileleji et al. (2006) employed commercial CO_2 sensors near the vents and exhaust air stream of fans in the grain bin for measuring CO_2. They concluded

that hot spot and early spoilage of grain can be detected inside grain bins using CO_2 sensors. Only few studies have been done to measure the intergranular CO_2 inside grain bulk (Muir et al., 1985) mainly because of lack of availability of sensors and deployment issues. Intergranular air temperature and air composition help to identify the location of spoilage inside the grain bulk. With the advent of novel polymer materials and micro-nanotechnology, CO_2 micro-sensors can be fabricated and deployed inside grain bulk to measure the intergranular air composition.

Carbon dioxide can also be used as a fumigant for insect control during grain storage. During fumigation, there is a need to measure the CO_2 concentration throughout the grain mass to ensure uniform distribution and maintenance of CO_2 concentration.

1.2 Dissolved CO_2 Measurement

Dissolved CO_2 is often measured in agricultural, food and bio-process industrial applications such as: food freezing, dry-ice production, photosynthesis process, aquaculture, waste water treatment, beverage and carbonated drinks manufacturing, cold storage, cargo ships, in-situ fermentation processes in a bioreactor, food processing environment, and bioprocesses monitoring. Additional potential application areas for CO_2 sensors in the agri-food industry are: ventilation control, industrial incubator monitoring, food transportation, food processing, food quality monitoring and storage of horticulture commodities.

Many traditional methods, processes and tools used in grain storage are continuously being replaced by automated systems and equipment because of the advancements in technologies. Rules and regulations by government agencies based on health and environmental concerns restrict the usage level of chemicals and insecticides in grain storage. Also, in order to address the aspects of quality assurance, continuous supply of grains as food and feed for society, and to meet the rising global standards, it is imperative for the agricultural and grain industry to adopt novel quality management systems to reduce losses and to maintain quality and safety during grain storage. Hence, there is a significant demand for novel sensors for measuring dissolved and gaseous CO_2 in the agri-food industry.

Global gas sensor market is US $320 million per year (MNT, 2006). The market revenue for gas sensors for the year 2009 is estimated to be US$3.8 billion (BCC Research, 2003; Frost & Sullivan, 2000). The Kyoto protocol and the increased awareness among the public about environmental pollution has fuelled sensors research and encouraged the need for novel CO_2 detectors (Coppock, 1998). The market potential for carbon dioxide (CO_2) sensors in the bulk food storage sector is huge, because the sensors can be used to detect incipient spoilage and to assess CO_2 levels in modified-atmosphere packages.

The general aim of my thesis is to identify the volatiles produced in wheat bulk, and develop and test a carbon dioxide sensor using PABA as the sensing material for grain quality monitoring. The specific objectives are to:

1) identify the volatiles produced in a wheat bulk by different combinations of *Aspergillus* spp., *Penicillium* spp., rusty grain beetle and red flour beetle;

2) a) develop and characterize a prototype sensor using PABA, hydrogel electrolyte and selective gas permeable membranes,

   b) select and evaluate CO_2 selective gas permeable membranes to be used in the construction of sensor,

   c) evaluate the developed sensor for the effects of temperatures, relative humidity, and presence of selected chemical compounds, and

   d) test prototype sensor for measuring varying gaseous CO_2 concentrations in small grain bulks and for the detection of dissolved CO_2 in liquids.

2. REVIEW OF CARBON DIOXIDE SENSORS

The term sensor is defined as a device or system including control and processing electronics, software and interconnection networks that respond to a physical or chemical quantity to produce an output that is measurable and is proportional to the quantity (e.g., gas concentration, ionic strength measurement) (Lees, 2003).

In general, most sensors consist of four major components, 1) a sampling area where the surface chemistry occurs, 2) a transducer, 3) signal processing electronics, and 4) a signal display unit. The two major functions in the gas sensing systems are the recognition of the molecule and transduction of that recognition event into a useful signal. The transducer helps in the conversion of one form of energy to another. The chemical reaction at the sampling area produces a change in a parameter such as pH, resistance, conductivity, or capacitance based on the exchange of electrons of ion reactions between the analyte and the surface material (Cattrall, 1997).

A number of sensing techniques have been proposed and developed for the routine measurement of CO_2 concentrations. The most common systems for CO_2 detection are: Severinghaus type potentiometric sensors (Severinghaus et al., 1958), gas chromatography (GC), mass spectrometers (MS) (Sipior et al., 1996), and infrared absorption detectors.

Severinghaus CO_2 sensor consists of a glass electrode filled with an aqueous bicarbonate solution and covered by a thin selective permeable membrane. This membrane is permeable to CO_2 but impermeable to water and electrolytes. The measuring principle is that in an aqueous solution, CO_2 forms carbonic acid which dissociates into a bicarbonate anion and a proton (Dieckmann and Buchholz, 1999). This process results in the pH-value change of an electrolyte solution which is measured by means of a pH-probe. Carbon dioxide is not measured directly, but in its ionic form. Additional disadvantages are that other volatile acid or basic gases impair the pH-value measurement and the maintenance costs are very high.

The working principle of GC is selective adsorption and elution of the gas molecules of interest. In MS, the sample gas is bombarded with a high energy electron beam causing fragmentation of the molecules in the sample. These fragmented molecules are made to move through an electric and/or magnetic field because of their charge and are separated based on their charge and mass (Karasek and Clement, 1988). Mass spectrometer is capable of producing measurements in near real time but it is very expensive, while GC is of low cost but requires much longer time to complete an analysis. Hence both GC and MS cannot be used for real-time measurements. Field portable miniaturized GC-MS are currently under development focusing on solving the instrumentation, miniaturization, deployment and sampling issues. A qualitative match purity of 75% is required for positive identification of compounds (CTEH, 2007). The level of mismatch between chromatographic peak signal purity and the mass

spectrometry peak signal decides the match purity of the GC-MS instrument. An ideal GC-MS should have peak impurities of not more than 0.05 to 0.1 percent.

2.1 Optical Sensors

The most commonly used CO_2 sensors are infrared detectors. Infrared detectors produce quick response times and are reliable but can only be used for gaseous CO_2 monitoring. Most of the commercially available CO_2 sensors (e.g., Model No. GMT220 Carbocap, Vaisala, Vantaa, Finland; Model No. TGS4160, Figaro Engineering Inc., Osaka, Japan; Model No.9510, Alphasense Ltd, Essex, UK) are non-dispersive infrared detectors (NDIR). The advantages of infrared gas sensors over analytical instruments such as GC-MS includes cheaper cost, compact size, easy process control, easy mass production and continuous measurement (Lee and Lee, 2001).

The non-dispersive infrared detector (NDIR) is simpler in structure and easy to use. The working principle is based on the energy absorption characteristics of CO_2 in the infrared region. All gases selectively absorb infrared light energy which corresponds to their own quantized vibrating energy. Carbon dioxide absorbs infrared radiation at wavelengths in the range of 2.7 to 15 μm (Skoog, 1985). In a typical NDIR sensor, infrared energy passes through two identical tubes (Figure 2.1). One is a reference tube and it is filled with non absorbing gas such as nitrogen. The second tube contains the gas sample to be analyzed and is a measurement cell. Filters or monochromators are used in the NDIR to obtain a monochromatic beam from an infrared light source with a wide wavelength

range. This light is allowed to pass through both the reference and the measurement cells. The gas in the measurement cell absorbs the infrared light, attenuating the energy which falls on the detector. This attenuated energy is compared to the unattenuated signal from the reference cell. The difference is proportional to the amount and the concentration of gas in the measurement cell.

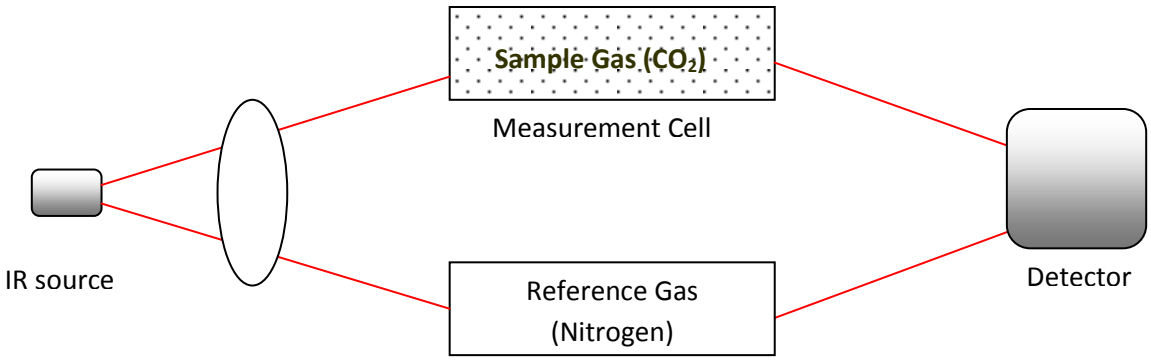

Figure 2.1 Schematic showing the working principle of a non-dispersive infrared carbon dioxide sensor.

Ion Optics (Santa Barbara, CA) has developed an optical platform technology for controlling and tuning the infrared emission and absorption wavelengths of a silicon surface using two-dimensional photonic crystals, produced through standard, high-volume, semiconductor manufacturing techniques. This technology has been employed in a silicon micro machined sensor chip for detecting CO_2 gas levels. The disadvantages of NDIR sensors are that they are bulky. Changes in the level of infrared energy in the system, source illumination

variation, light scattering from particulates and thermal drift are some of the measurement errors in the NDIR sensors (Kinkade, 2000). Regular calibration with zero gas such as nitrogen becomes essential for accurate measurements. The weatherproof cover or the probe tubing becomes necessary for gas sampling. Detection of CO_2 sensing based on its strong absorption in the infrared region has further disadvantages of interference from water vapour and carbon monoxide (Herber et al., 2005).

2.2 Fiber Optic CO_2 Sensors

Fiber optics is another optical method for detecting CO_2. These types of sensors are called optodes. Fiber optic sensors contain a chemical sensing layer at the tip of a fiber which changes optical properties in response to CO_2.

Optical fiber based CO_2 sensors have been fabricated by several researchers (Colin et al., 2003; Segawa et al., 2003; and Nakamura and Amao, 2003) using materials showing absorbance or reflectance changes on exposure to CO_2. The sensing elements such as pH indicating organic dyes or organometallic complexes supported in gas-permeable polymer films have been used. When the sensing element is exposed to CO_2, it creates a change in absorbance or reflectance of the film. After exposure, the sensing spot is examined by an amber LED (light-emitting diode) with peak emission at specified wavelength corresponding to the basic form of the reagent. The LED light shining through the film generates heat at the spot by the non-radiative decay of excited states, resulting in an expansion of the spot and a stress on the polymer film. This

creates a charge on the film and the charge is correlated with the concentration of CO_2 gas.

Mulroney et al. (2006) developed a fiber optic CO_2 sensor using a pyroelectric detector coupled to the chalcogenide fiber which converts the changes in incoming infrared light to electric signals. Pyroelectric materials are characterized by having spontaneous electric polarization, which is altered by temperature changes as infrared light illuminates the elements. Pyroelectric CO_2 detectors are suitable for only room temperature operation.

The advantage of a fiber optic gas sensor is that it is chemically inert and not cross-sensitive to the presence of other gases in the background. A fiber optic gas sensor has the drawback of using lenses which results in interference of transmission of light over time because of dust or soot coating. Hence, a fiber optic sensor needs frequent cleaning of lenses for continuous functioning. Expensive advanced readout equipment is necessary to sense the change at the tip of the fiber.

2.3 Sol-Gel Optical Sensors

Bultzingslowen et al. (2002) fabricated an optical sol-gel based CO_2 sensor strip using fluorescent pH indicator. The sensor membrane consists of a ruthenium dye incorporated in polymer nano-beads and by means of ratiometric method, the analyte-sensitive fluorescence intensity signal is measured. This sensor strip can be located inside the food package and can be sampled by a hand-held scanning device from the outside using wireless technology.

2.4 Electrochemical Sensors

To address the need for compact sensors in space research, fire detection, emission monitoring in aerospace applications, medicine and biology, considerable research is being carried out using nanotechnology and microelectronics to enhance the performance of sensor devices. All chemical sensors depend on interactions occurring at the atomic and molecular level. Both nano and MEMS (micro-electro-mechanical systems) technologies provide ways to measure variables that until recently were too difficult or too expensive to sense. Hence the potential of nanosensors and nano-enabled sensors is promising in gas sensing applications (Nagel and Smith, 2003). Substantially smaller size, lower mass, more modest power requirements, greater sensitivity, and better specificity are the potential benefits of exploiting microelectronics and nanotechnology in sensor fabrication.

Electrochemical or solid state electrolyte sensors are the most predominantly available sensors which make use of the MEMS and nanotechnology for CO_2 monitoring. These sensors can be classified into potentiometric, amperometric, and conductometric based on the measurement method. In the potentiometric mode, the measured signal is an electromotive force, while in the amperometric mode an electric current is recorded. In the case of conductometric sensors, the current–voltage plot is analysed. The materials used for construction of the sensors are selected based on their ability to withstand the extreme conditions such as high temperature and corrosive media, in the agri-food industry.

Based on the variety of principles (potentiometric, amperometric, or conductometric) and materials (metal oxides, polymers, ceramics or sol-gel), solid state sensors are the best candidates for the development of commercial gas sensors (Capone et al., 2003; Moseley, 1997). Solid state electrolyte sensors have numerous advantages such as small sizes, high sensitivity in detecting very low concentrations (at level of ppm or even ppb), possibility of on-line operation and, low cost possiblly due to large-scale production. But these types of sensors also suffer from limited measurement accuracy and problems of long-time stability.

2.5 Metal Oxide Sensors

A metal oxide gas sensor consists of a sensitive layer (sensing material) deposited over a substrate provided with electrodes for the measurement of the electrical characteristics. The sensor element is heated by its own heater which is separated from the sensing layer and the electrodes by an insulating layer (Figure 2.2). This heating element can be a platinum or platinum alloy wire, a resistive metal oxide, or a thin layer of deposited platinum. The electrodes connect to the sensing material to form a closed-loop circuit.

The mechanism of gas detection of metal oxide sensors is based on the chemical reactions that occur on the sensor surface. In the presence of gas, the metal oxide causes the gas to dissociate into charged ions or complexes which results in the transfer of electrons. The electrons become available or unavailable due to oxidation or reduction causing conductance or resistance of the surface

layers to change upon exposure to the analyte. The change in conductivity (or resistivity) vs gas concentration can be measured in the metal oxide sensors. This change in conductivity is directly related to the amount of CO_2 present in the environment, resulting in identification and quantitative determination of the gas concentration. The built-in heater, which heats the metal oxide material to an operational temperature range that is optimal for the gas to be detected, is regulated and controlled by a specific circuit (Datta, 1992; Barsan and Weimar, 2001). A pair of biased electrodes is imbedded into the metal oxide to measure its conductivity or resistivity change. Typically the sensor will produce a very strong signal at high gas concentrations.

Mahmoudi et al. (2007) have demonstrated that porous silicon coated with hydrocarbon groups (CHx) annealed at different temperatures can emit a blue light in response to CO_2 gas. Stabilization of the photo luminescent properties of the porous silicon in an actual sensor device has not yet been established and is undergoing further research.

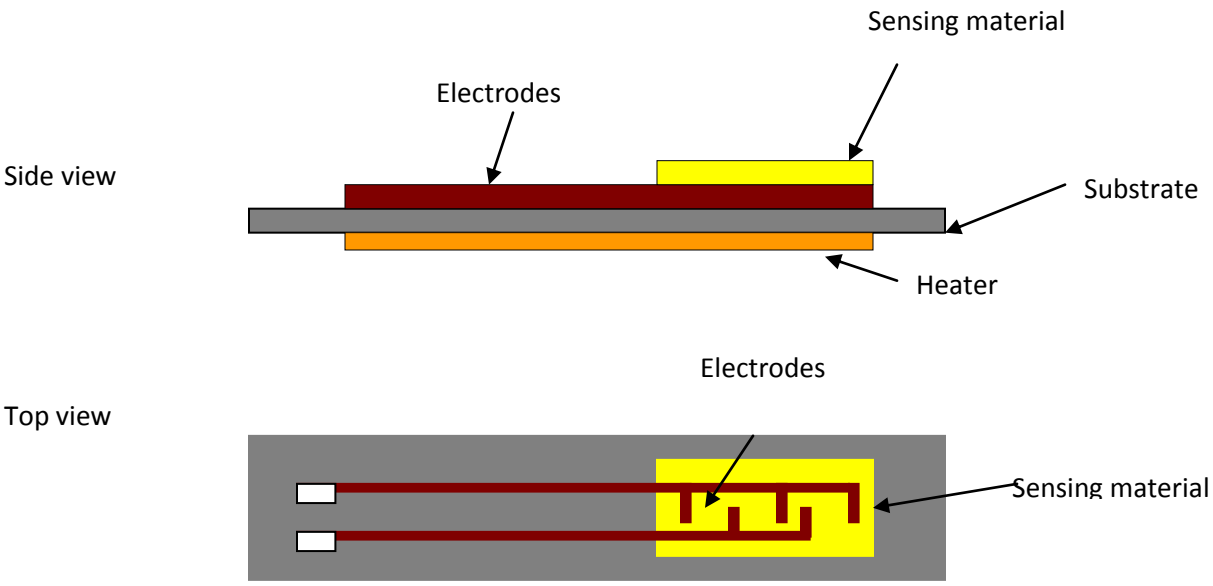

Figure 2.2 Schematic showing components used in a typical metal-oxide sensor.

Resistive metal oxide gas sensors are expected to generate revenues of US $2.5 billion by 2010 (Hooker, 2002). In the MEMS based microelectronics sensor design, selection of sensing material is an essential criterion. Several materials have been reported to be used as sensing material for detecting CO_2 (Table 2.1)

Table 2.1 Characteristics of metal oxide sensor materials for detecting CO_2.

Types of sensing materials	Detection range	Operating temperature (°C)	Reference
$BaTiO_3$–CuO	0–2000 ppm	400	Mandayo et al. (2006)
LaOCl and SnO_2	400–2000 ppm	350–550	Diagne and Lumbreras (2001)
$LaCl_3.7H_2O$ – SnO_2	0 to 2500 ppm	400	Kim et al. (2000)
CrO-BaTiO3-	0 to 7%	700	Haeusler and Meyer (1996)
La203--CaCO3			
CuO-$BaTiO_3$ and NiO-$BaTiO_3$	100 to 6000 ppm	800	Ishihara et al. (1991)

2.6 NASICON Sensors

NASICON powder ($Na_{2,8}Zr_2Si_{1,8}P_{1,2}O_{1,2}$) has been proposed to be used as a promising solid electrolyte in electrochemical sensing of CO_2. High ionic conductivity, high chemical stability and the less influence of humidity on NASICON makes it a preferred material for CO_2 sensing (Jasinski et al., 2006). Several researchers (Zhu et al., 2005; Pasierb et al., 2004) around the world including National Aeronautics and Space Administration (NASA), United States

have proposed that NASICON is the best sensing material for CO_2 sensors (Table 2.2).

The advantages of semiconducting metal oxide gas sensors over competing technologies such as conducting polymers, electrochemical and quartz crystal are robustness and long term stability (Williams and Pratt, 2001).

Most commercially available microfabricated sensors (e.g., Cole-Palmer, Chicago, USA; Figaro Engineering Inc., Osaka, Japan) are made of a substrate heated by wire and coated with a metal oxide, semiconducting film. The sensors rely on the changes of conductivity induced by the adsorption of gases and subsequent surface reactions. These micromachined sensors operate at a relatively high temperature of 200–450°C which results in significant power consumption. The sensors cannot function without small heaters (usually platinum or gold) on the back side to keep the sensors at operating temperatures. Because of the high operating temperatures, metal oxide sensors are inappropriate in potentially flammable environments (Dickinson et al., 1998) or explosive environment such as grain stores. Metal oxide based gas sensors are not recommended to monitor quality of food because irreversible binding of sulphur compounds may cause poisoning (Schaller et al., 1998). The output of the metal oxide gas sensors varies logarithmically with the gas concentration. This limits the accuracy of the sensor and the overall measurement range of the sensor. Metal oxide sensor performance can also be affected by device cross-sensitivity to environmental factors such as temperature and humidity. Though

the metal oxide sensors are relatively low in cost, the stability and repeatability of the sensor is poor.

Table 2.2 Characteristics of NASICON sensing materials for detecting CO_2.

NASICON sensing material	Detection Range	Operating Temperature (°C)	Reference
NASICON/ Li_2CO_3 - $BaCO_3$	100-1000 ppm	345	Zhu et al. (2005)
NASICON/ Li_2CO_3 - $BaCO_3$	500 – 12600 ppm	475	Pasierb et al. (2004)
NASICON/ Na_2CO_3 - Ba_2CO_3	0-4%	425	Ward et al. (2003)
NASICON/ Na_2CO_3 - Ba_2CO_3	6 ppm – 100%	600	Wang and Kumar (2003)
NASICON/ Li_2CO_3	350-1000 ppm	450	Kaneyasu et al. (2000)
NASICON/Perovskite oxides	100-2000 ppm	300	Shimizu and Yamashita (2000)
NASICON	0-5%	450	Yang and Liu (2000)
NASICON/ Li_2CO_3 - $BaCO_3$	300-5000 ppm	400	Lee et al. (1995)

2.7 Polymer Sensors

The advantage of a polymer-based gas sensor over metal oxide sensors is that polymer films are capable of broadly detecting and identifying various constituents in the air in addition to the target analyte. Polymer films are multifunctional, useful, economical, and practical in a wide range of applications and sensor designs. In addition, miniaturization of microelectronics favors the use of polymer thin films in sensors.

Carbon dioxide sensors fabricated using polymer materials are mostly miniaturized version of the Severinghaus CO_2 probe (Severinghaus and Bradley, 1958). Severinghaus CO_2 probe consists of a glass electrode filled with an aqueous bicarbonate solution and covered by a thin plastic membrane. This plastic membrane is permeable to CO_2 but impermeable to water and electrolytes. The measuring principle is based on the concept that in an aqueous solution, CO_2 forms carbonic acid, which dissociates into a bicarbonate anion and a proton. This process results in a pH-value change of the electrolyte solution, which is measured by the glass pH probe.

Cui et al. (1998) developed a potentiometric pH sensitive CO_2 gas sensor system using polyaniline deposited platinum electrodes for aqueous phase environment. This sensor had the drawback of being sensitive to dissolved oxygen. Modifications using a gas-permeable membrane and reference electrodes are necessary before making this sensor usable for gas phase applications. Potentiometric sensors measure a change in voltage and are

shielded and susceptible to line noise and other interferences. Amperometric sensors measure a change in current as a response to analyte and are simpler in structure without gas sealing. The potentiometric method is not always suited to monitoring small variations of gas concentration, since the response signal is usually linear to the logarithm of gas concentration. In contrast, an amperometric type sensor produces a sensing signal proportional to the gas. Hence amperometric sensors are preferred over potentiometric sensors for food quality monitoring due to the linear and reliable sensing in narrow concentration regimes.

Takeda (1999) demonstrated that plasma polymerized polyaniline thin film deposited on gold electrodes showed an increase in conductivity upon exposure to 100% CO_2 gas in comparison with dry air. The results of this study can be taken only as a proof of concept as the researchers did not test the thin films to various CO_2 concentration levels.

Ogura and Shiigi (1999) demonstrated a linear relationship between the electrical conductivity of a composite film prepared from heat treated poly (aniline anthranalic acid) (PANA) and poly (vinyl alcohol) (PVA) to CO_2 concentrations of up to 10,000 ppm. Irimia-Vladu and Fergus (2006) developed a CO_2 sensor using the procedures of Ogura and Shiigi (1999) and found out that the response of the heat-treated PANA and PVA composite thin film was slow and smaller in magnitude with severe drift and unacceptable long response time. The absence of the sensor's response is consistent with other report (Warren et al., 1989)

indicating that the onset of protonation in emeraldine base occurs only when the pH level of the protonating bath is lowered below 4. The protonation mechanism proposed by Ogura and Shiigi (1999) is not consistent with the reported conductivity characteristics of polyaniline.

Oho et al. (2002) (Ogura group) demonstrated that the logarithmic ac impedance of the base-type PANA/PVA composite was linearly related to the log of CO_2 concentration at up to 80% humidity. As the response signal value of the sensor is linear to the logarithm of gas concentration, this sensor may not be suitable for monitoring small variations of gas concentrations.

Tongol et al. (2003) fabricated a potentiometric pH-indicating polypyrrole based CO_2 sensor. Carbon dioxide diffusing through the polypyrrole membrane forms carbonic acid which dissociates and alters the pH of the internal electrolyte. This potentiometric probe made of bicarbonate-doped polypyrrole membrane as a pH-sensing element was used for detecting the changes in CO_2 concentrations. An X-ray photoelectron spectroscopy analysis showed that the material displayed poor repeatability and reproducibility of potentiometric responses. Waghuley et al. (2008) developed a polypyrrole CO_2 sensor using a screen printing technique. The resistance value of the sensor showed linear variation with an increase in CO_2 concentration but a saturation effect was observed above 700 ppm. Hence polypyrrole may not be a good candidate for detecting higher concentrations of CO_2.

Suzuki et al. (2000) have developed a Severinghaus type metal oxide CO_2 sensor using iridium oxide film as the pH sensing element for blood-gas analysis applications. This sensor needs further modification using electrolyte to be used in real time applications. The issue of cross-sensitivity is not addressed by these researchers and the practical implementation of a CO_2 sensor in the agri-food industry needs selective gas permeable membranes to avoid cross sensitivity to other gases. For an ideal food quality monitoring CO_2 sensor, the sensor's performance criteria including sensitivity, selectivity, effect of interference (temperature and humidity), repeatability, reversibility, hysteresis effect and drift of the sensor need to be studied and characterized.

2.7.1 PABA based CO_2 sensor

In a pH-based CO_2 sensor, the operating pH range is near neutral (6.5 to 7.5 pH range). But polyaniline is not electro active above pH 3 (Irimia-Vladu and Fergus, 2006). So, it is not possible to use polyaniline as a sensing material for real-time pH-based gaseous and dissolved CO_2 sensing. Self-doped conducting polyanilines overcomes this issue of working range of pH for CO_2 sensing. In self-doped polyanilines, the negatively charged anions like sulfonate, carboxylate or phosphonate covalently attached to the polymer backbone, act as intramolecular dopant anions which are able to compensate positive charges at protonated nitrogen atoms on the polymer backbone, thus replacing auxiliary solution dopant anions (Freund and Deore, 2007). These polymers are water soluble and electroactive and can be conducting over wider pH ranges. The syntheses of

self-doped sulfonated polyanilines have been mostly carried out by post-modification of polyaniline with strong acids.

The electrochemical polymerization of sulfonate, carboxylate or phosphonate substituted polyanilines is slow and time consuming. Self-doped poly aniline boronic acid (PABA) can be synthesized and processed in aqueous and non-aqueous media and it is electroactive at neutral and above neutral pHs (Deore et al., 2004). The formation of anionic tetrahedral boronate ester in saccharides and alcohols in the presence of fluoride forms the basis of self-doped soluble PABA.

The PABA has been used as a promising sensing material for developing (i) a saccharide sensor (Shoji and Freund, 2002); (ii) a conductometric sensor for dopamine detection (Fabre and Taillebois, 2003); and (iii) an amine vapour detection sensor (English et al., 2006). The electrochemical potential of the polymer PABA is sensitive to changes in the pKa (acid dissociation constant) of the polymer as a result of its interaction with change in analyte concentrations (Shoji and Freund, 2002). The pH-dependent equilibria of PABA and its similarity in sensitivity to pH changes as that of polyaniline has been studied by Deore et al. (2006) and Deore and Freund (2009).

In this work, self-doped PABA dispersion which is electroactive and conducting under neutral and basic conditions due to the formation of boron-phosphate complex containing fluoride has been used as the sensing material. The added advantages of using PABA as a sensing material for CO_2 detection are: the ability to be used as a simple physical dispersion process for electrode

deposition, high environmental stability, and its water solubility during electro-chemical polymerization. As the polymerization occurs in a water-based solvent, it helps to avoid processing problems during large-scale sensor manufacturing.

3. IDENTIFICATION OF VOLATILE METABOLITES IN STORED-GRAIN HEAD SPACE FROM MULTIPLE SPECIES

Grain odors are caused by complex mixtures of compounds having various degrees of volatility. Volatiles can come from the grain itself, fungi or insects. Although numerous insect and fungal species can occur within a grain bulk, *Aspergillus* and *Penicillium* genera of molds and rusty grain beetle (*Cryptolestes ferrugineus*) and red flour beetle (*Tribolium castaneum*) insects are the common in Canadian grain (White, 1995). Fungi can produce a series of alcohols (3-methyl-l-butanol, 1-octen-3-ol, 1-octanol and 3-octanone) in bulk wheat (Sinha et al., 1988). The rusty grain beetle, *Cryptolestes ferrugineus* produces a mixture of 4, 8-dimethyl-E, 4,8-decadienolide and ferrulactone II in grain bins (Loschiavo et al., 1986). Flour beetles (*Tribolium* species) produce functionalized aromatics e.g., 1,4-dimethoxybenzene, 2-methyl-1, 4-dimethoxybenzene and 2-ethyl-1,4-dimethoxybenzene (Seitz and Ram, 2000). Previous studies (Seitz and Ram, 2000; Loschiavo et al., 1986; Sinha et al., 1988) have identified and detected odours in stored wheat infested by single species of fungi or by a single insect. Co-occurrence of insect species and moulds is common in a stored-grain ecosystem and both can cause grain spoilage. The materials and methods to identify volatile compounds evolving from grain having a combination of moulds and insects are described in this section.

3.1 Materials and Methods

3.1.1 Samples

Canada Western Red Spring (CWRS) wheat (variety AC Superb), conditioned to 14, 16.5 and 19% moisture content (m.c.) was used in this study. A total of 10 combinations of insect infestations and fungal infections were used. These were: (1) *Aspergillus niger van* Tieghem, (2) *Penicillium spp*, (3) rusty grain beetle, (4) red flour beetle, (5) *A. niger* and *Penicillium* spp., (6) *A. niger* and rusty grain beetle, (7) *A. niger* and red flour beetle, (8) *Penicillium* spp. and rusty grain beetle, (9) *Penicillium* spp. and red flour beetle, (10) rusty grain beetle and red flour beetle. A total of 3 replicates were done for each type of infestation. The infestation types (1), (2), (3) and (4) were used for comparing the results with published literature. Three jars of wheat at 14% m.c. were used as control samples. Two kilograms of wheat samples were stored in each of the 99 glass jars of 4 L capacity (10 combinations X 3 replicates X 3 moisture content levels + 3 controls X 3 replicates).

3.1.2 Infestation procedure

The commonly occurring grain storage fungi, *A. niger* and *Penicillium* spp. were cultured from naturally infected wheat kernels. Wheat kernels with the fungi were placed on filter paper saturated with 7.5% aqueous NaCl in petri dishes separately for 7 d. The pure fungal lines were placed on potato dextrose agar (PDA) for one week at 30°C. The PDA was placed in sterilized water with one drop of Tween 20. Approximately 50 kg composite sample of CWRS wheat at

17% m.c. (wet basis) was sterilized by soaking in 1% sodium hypochlorite for 2 min and then rinsed thoroughly with distilled water. The sterilized wheat kernels were sprayed with the water containing cultured *A. niger* fungi. Another 50 kg of wheat sample was also infected with *Penicillium* spp. using the above procedure.

To determine the effect of presence of insects on odour volatiles, jars containing wheat were infested with 500 rusty grain beetles and 100 red flour beetles. Different insect counts were chosen based on consultation with entomologist Dr. White at the Cereal Research Centre, Agriculture and Agri-Food Canada. Rusty grain beetle look very much like the red flour beetle but are about one-tenth the size of the flour beetles. The body mass of the insects were considered (1 live rusty grain beetle adult = 0.2 mg; 1 live adult red flour beetle = 2.0 mg) in infesting the wheat jar. Wheat and control samples were stored at 30°C and 75% r.h. for six weeks. After six weeks, a sub-sample was taken from each jar and used for the collection of volatile organic compounds.

3.1.3 Collection of volatile organic compounds

The experimental setup for trapping volatile metabolites is shown in Fig 3.1. Headspace volatiles produced by the infested wheat were collected using a setup, with modifications recommended by Sinha et al. (1988). Sub-samples of infested wheat (200 g) were placed in a 500 ml conical flask fitted with a two-holed rubber stopper containing glass tubes. One glass tube was placed just 1 cm above the bottom of the jar inside the infested wheat bulk with the other end connected to a nitrogen supply system. The end of the second glass tube was

positioned near the neck of the flask with the other end connected to a volatile trap. The volatile trap was made of glass tube (75 mm X 3.5 mm i.d.) packed with 200±10 mg of Johns-Manville Chromosorb 105, 60/80 mesh adsorbent (Denver, CO). Before use, the traps were placed on a 150 mm Petri plate, wrapped with aluminum foil, and sterilized at 150°C for 2 h. The neck of the conical flask was tightly sealed with Parafilm to prevent the escape of volatile organic compounds. The stream of 99.99 % N_2 was maintained at 100 ml min^{-1} for up to 17 h. The volatiles in the adsorbent were eluted into glass vials with 0.5 ml of methylene chloride.

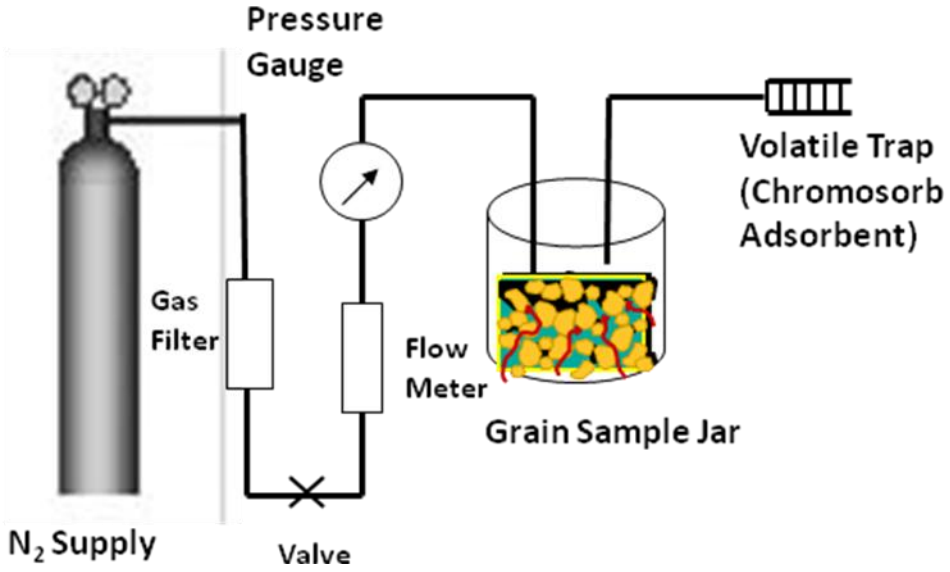

Figure 3.1 Schematic showing the experimental setup for trapping volatile metabolites.

3.1.4 GC–MS analysis of the volatiles

Gas chromatography (GC) was performed using a Varian Star 3400 CX series GC (Varian Inc., CA, USA) with a flame ionization detector, available in the Department of Chemistry, University of Manitoba. The samples were separated on a 15 m DB-1 mega bore column of 100% dimethylpolysiloxane (Sinha et al., 1988; Fernando et al., 2005). The trap contents were adsorbed at 22°C from a uni-injector onto a fused silica column (BP1, 25 m length × 0.22 mm i.d., 0.25 µm film thickness), which was cryogenically focused with dry ice and acetone for 2 min. The column was attached to a Hewlett-Packard 5890 Gas Chromatograph (Hewlett-Packard, CA, USA) attached to a Hewlett-Packard mass selective detector. Helium was used as the carrier gas with a flow rate of 6 ml min^{-1}. The injector and detector temperatures were maintained at 200°C and 250°C, respectively. The oven temperature program was 37°C for 0.5 min, raised to 77°C at a rate of 20°C per min, held at 77°C for 5 min, raised to 150°C at a rate of 2°C min^{-l}, and held at 150°C for 10 min. The mass spectra of the unknown compounds were compared with those in the NIST/EPA/NIH Mass Spec. Library (Version 2.0) (Gaithersburg, MD, USA).

GC-MS analysis spectra of control samples (pure wheat) were used as background to subtract for identifying the compounds from all types of infested samples.

4. MATERIAL PREPARATION AND SENSOR ASSEMBLY

4.1 Carbon Dioxide Gas Concentrations

The correlation between different ppm levels of CO_2 and indication of infestation in grain stores has been established by Semple et al. (1988) (Table 4.1). Instruments capable of sensing CO_2 concentrations of 0.1% (1000 parts per million) in air in grain bulk will detect deterioration in 80% of deteriorating bulks in farm granaries (Muir et al., 1985).

Simulation models of Singh (Jayas) et al. (1983) and experimental data of Muir et al. (1985) concluded that in the absence of prior knowledge of the location of potential deterioration of grain, a sensor capable of detecting CO_2 levels of 2 g/m^3 should be located near the centre of the bin. Using the following equation (Semple et al., 1988) the CO_2 concentration be converted to part per million by volume:

$$ppmv = \frac{\left(\frac{mg}{m^3}\right)(273.15+°C)}{(12.187)(MW)} \qquad (1)$$

where, ppmv = ppm by volume (volume of CO_2 per 10^6 volumes of ambient air)

mg/m^3 = milligrams of CO_2 per cubic metre of ambient air (2000 mg/m^3)

°C = ambient air temperature in degrees centigrade

MW = molecular weight of CO_2 (44.01)

At 25°C, ppmv = 1111.77.

Hence, for grain quality monitoring, the carbon dioxide sensor should be able to measure at least 1112 ppm to detect incipient grain spoilage.

Table 4.1 Carbon dioxide concentrations as an index of infestation in grain stores. Source: Semple et al. (1988)

CO_2 Concentration (ppm)	Indication of infestation
380 to 500	Atmospheric concentration (no spoilage)
<1100	Incipient spoilage
1100 to 3500	Slight insect infestation and (or) infestation of microorganisms
3500 to 5000	High insect infestation and (or) a higher infection of microorganisms
5000 to 9000	Severe spoilage and limit of dangerous storage conditions
>10000	Highly unsuitable storage conditions

4.2 Instrumentation

4.2.1 Gas flow management system

A proper gas flow management system is crucial for successful sensor characterization. The gas flow management and the sensor evaluation system consists of a flow system to control the desired gas flow rates to the Teflon testing chamber, and a data collection system to record data from the sensor.

An automated vapor delivery system was custom built by Plasmionique Inc., St Hyacinthe, PQ which can produce up to 8 vapors from solvents that are stored in 8 different glass bubblers. The flow rate of the vapors can be controlled using mass flow controllers and solenoid valves and be delivered to a Teflon gas mixing chamber and then delivered to the sensor-testing chamber. This system allows the user to produce mixtures of analyte at various flow rates and at desired concentrations of analyte solutions. The automated gas flow management system affords several advantages including unattended operation during long sequences of tests, reduced user exposure to toxic chemicals and precise data measurements. This automated system provides enough flexibility and capabilities to allow the users to build and design experiments with applications without the concern of limitations and / or expansion capabilities. This custom built automated vapor delivery system was used for characterizing the developed CO_2 polymer sensors. A schematic of the custom built gas flow management system (Plasmionique Inc., St Hyacinthe, PQ) is shown in Figure 4.1.

4.2.2 Data collection system

The data collection system used for characterization of the CO_2 sensor consists of an Agilent 34980A Data Acquisition Switch Unit (Agilent Technologies, Inc., Santa Clara, CA). The dc resistance of the sensor was read sequentially by the Agilent data acquisition unit. The control computer was interfaced with data collection system through an IEEE general purpose interface board (GPIB). The resistance data were initially stored in the data acquisition unit and once a complete set of data were recorded, the GPIB communications protocol sent the data to the control computer where the data were stored in a tab-limited text file. The gas flow management system and the data collection system were interlinked and connected through a LabVIEW (National Instruments Corporation, Austin, TX) algorithm to efficiently control and simultaneously record the gas mixture readings and the sensor response output values.

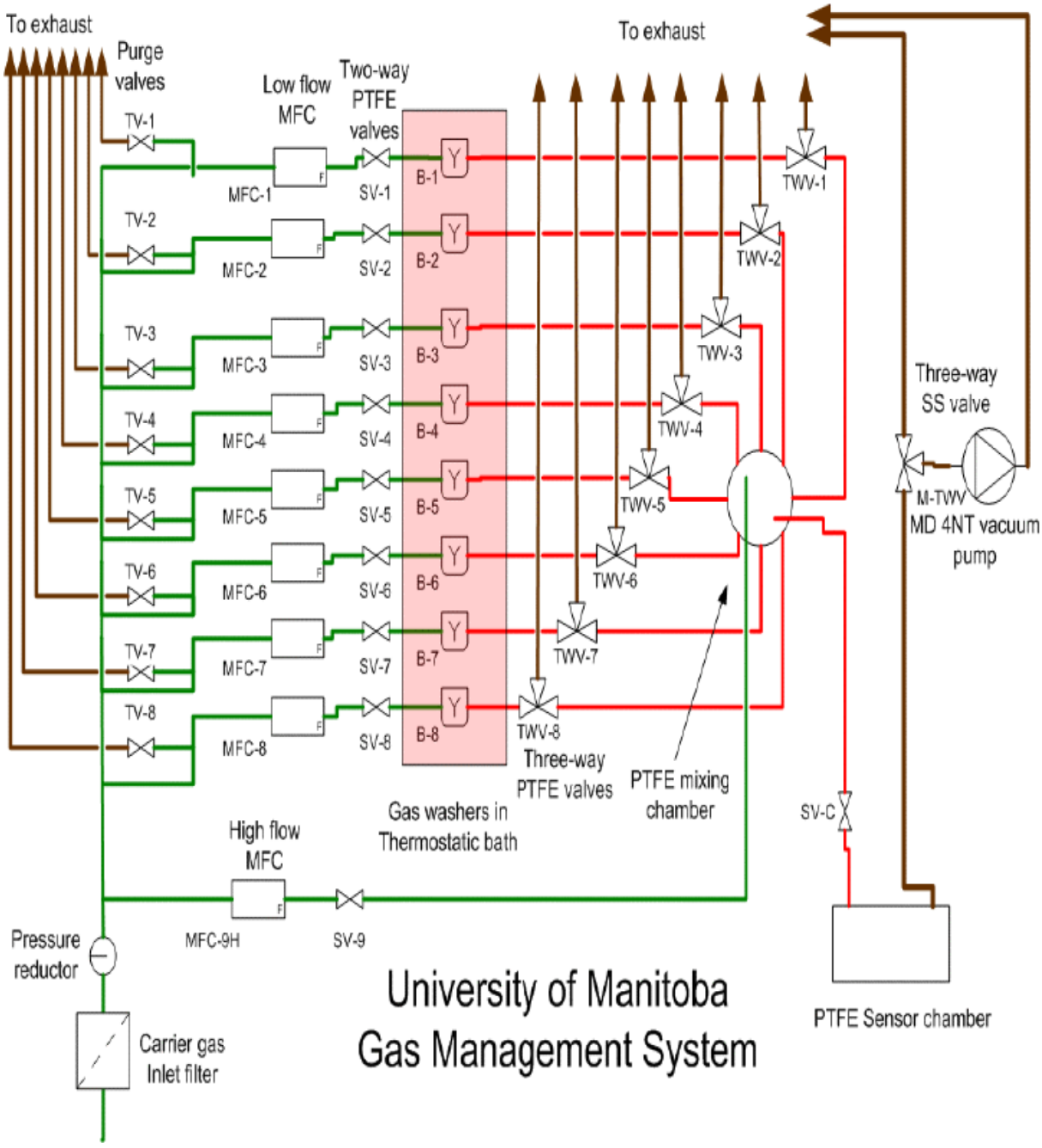

Figure 4.1 Schematic diagram of the Gas Management System. Source: Plasmionique FLOCON Vapor delivery system manual.

Commercially available gas cylinders (Praxair, Edmonton, AB) with a blend of CO_2/air mixture of 9820 ppm concentration and a nitrogen cylinder of ultra high purity (99.99%) were used for the measurements. To achieve the required ppm levels of CO_2 concentrations, gas from 9820 ppm level was diluted to appropriate concentrations by mixing and varying the gas flow rate from the nitrogen cylinder. For example, a flowrate of 100 sccm of 9820 ppm and 100 sccm of nitrogen in the Teflon mixing chamber measured at the same pressures and temperatures produced 200 sccm of 4910 sccm of CO_2 (Table 4.2). In a similar fashion, desired levels of CO_2 concentrations were achieved by mixing various levels of nitrogen and CO_2 from a 5000 ppm CO_2 in air.

Table 4.2 Gas flow mixture ratio of nitrogen (99.99%) and carbon dioxide (9820 ppm) to achieve desired CO_2 concentrations. X indicates the flow rate of nitrogen inside bubbler containing water.

MFC 8 (sccm) (CO_2)	MFC 9 (sccm) (N_2)	MFC 1 (sccm) (N_2 through water)	CO_2 ppm
7.8	192-X	X	382
20	180-X	X	982
30	170-X	X	1473
50	150-X	X	2455
60	140-X	X	2946
75	125-X	X	3682
100	100-X	X	4910

The sensor to be characterized was placed inside a custom made Teflon (PTFE) sensor testing chamber and, exposed to the gaseous mixtures of CO_2 in nitrogen delivered via the gas flow management system. Figure 4.2 shows the schematic of the PTFE testing chamber.

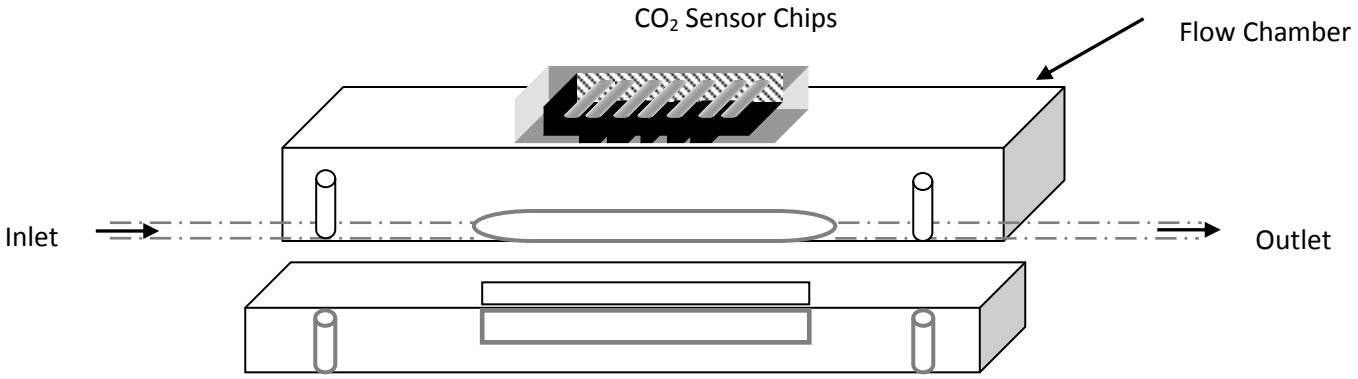

Figure 4.2 Flow cell cartridge for the sensor characterization for CO_2 measurement.

4.3 Materials

The reagents, chemicals and adhesives including 3-aminophenylboronic acid, poly aniline, phosphoric acid, sodium fluoride, ammonium persulfate, poly vinyl alcohol, potassium chloride, nafion, cyanoacrylate (Permabond 105), poly vinyl chloride, used for the sensor construction were of analytical grade and purchased from Sigma-Aldrich Inc (St. Louis, MO). All aqueous and buffer solutions were prepared with 18.2 MΩ quality deionized water using an ultrapure water system (Millipore Corporation, Billerica, MA). Carbon dioxide porous PTFE membranes with 60 µm thickness and with average pore diameter of 0.2 µm were acquired from Thermo Scientific (Waltham, MA). Chemically resistant perfluoroelastomer O-rings of 0.3 mm diameter and 0.1 mm wall thickness used for mounting the PTFE gas permeable membrane were purchased from Fisher Scientific (Pittsburgh, PA).

4.4 PABA Film Synthesis

Poly aniline 3-boronic acid (PABA) film was synthesized according to established procedures (Deore and Freund, 2009). The PABA dispersion solution was synthesized chemically using 10 mM 3-APBA (monomer) + 50 mM NaF + 5 mM ammonium persulphate (oxidant) in 0.1 M phosphoric acid. The chemical synthesis of PABA polymer is easily water dispersible, and hence it facilitates to form smooth, adherent and uniform thin films on the electrode surface. The particle size of PABA is in the range of 50-100 nm and provides a higher surface area for sensing.

4.5 Sensor Construction

A cross-sectional and a schematic side view of the constructed sensor assembly are shown in Figures 4.3 and 4.4, respectively. Gold interdigitated array electrodes (IDAs) to be used as the sensor substrate platform, deposited on a 1 mm thick printed circuit board (PCB) was custom designed upon consultation with Iders Inc, Winnipeg, MB. The sensor chip was fabricated by Dynamic & Proto Circuits Inc, Stoney Creek, ON. Each sensor chip has seven sensor elements (detectors) (Figure 4.6). The dimensional details of the interdigitated electrode are shown in Figure 4.5.

The PABA was used as the sensing material in preparing the electrically conductive region for the sensor. A 2 µL PABA solution was deposited on the IDAs through a micropipette as a physical dispersion process and was allowed to

dry for 20 min. A 2 µL of Nafion solution was superimposed directly on top of the PABA thin film in the electrically conductive region of the sensor. The solution was then allowed to evaporate in air at 25°C and a dried residue was left to form the conductive sensing material.

Similarly, an internal electrolyte-hydrogel solution prepared from an aqueous solution of 99.99% hydrolyzed polyvinyl alcohol (0.5 wt/vol %) with 0.0001 M sodium bicarbonate and 0.0001 M potassium chloride was also used for building the sensor assembly. A 4 µL of the internal electrolyte/hydrogel composite was superimposed directly on top of the PABA thin film in the electrically conductive region of the sensor. The solution was allowed to evaporate and a dried residue was left to form the ion-selective gas permeable membrane.

The PTFE membrane was applied directly on top of the dried residue of the internal electrolyte (Nafion or PVA electrolyte-hydrogel membrane) with the aid of an O-ring. The membrane was cut into circular shapes of approximately 11 mm diameter and was attached to the O-rings by applying small amounts of cyanoacrylate adhesive. The O-ring with the mounted membranes was glued carefully to the PCB substrate of the sensor assembly, forming a cavity with the electrolyte/hydrogel composite and the PABA thin film below the membrane. Care was taken to apply the adhesive only on the rim of the O-ring and thereby avoiding the adhesive contact with the sensing material. The gap between the gas permeable membrane and the surface of the electrolyte/hydrogel composite

was kept at a minimum distance (<0.2 mm) using an O-ring to maintain the thin layers of the electrolyte and sensing material.

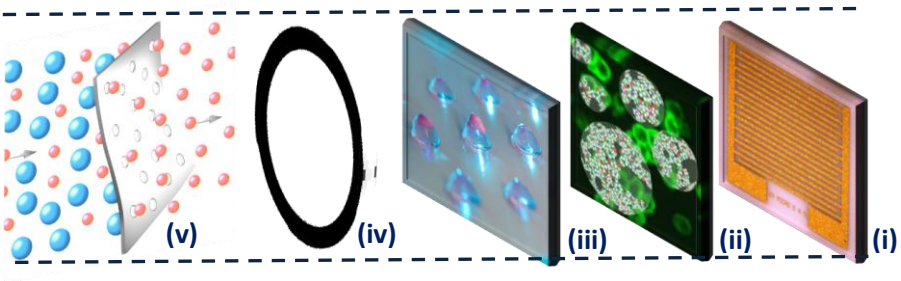

Figure 4.3 Pictorial cross-sectional view of the CO_2 sensor (i) Gold interdigitated electrode PCB array, (ii) PABA polymer, (iii) Nafion, (iv) O-ring, (v) Gas permeable membrane.

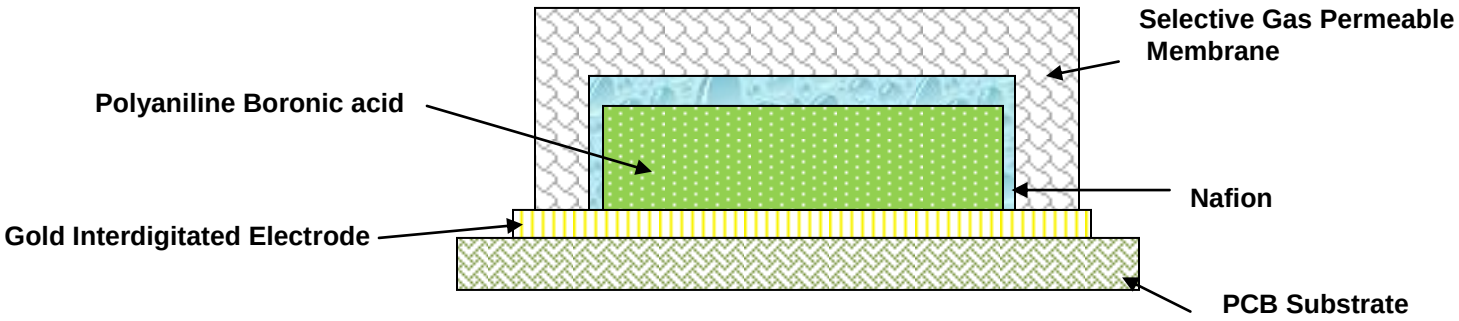

Figure 4.4 Schematic side view of the constructed CO_2 sensor.

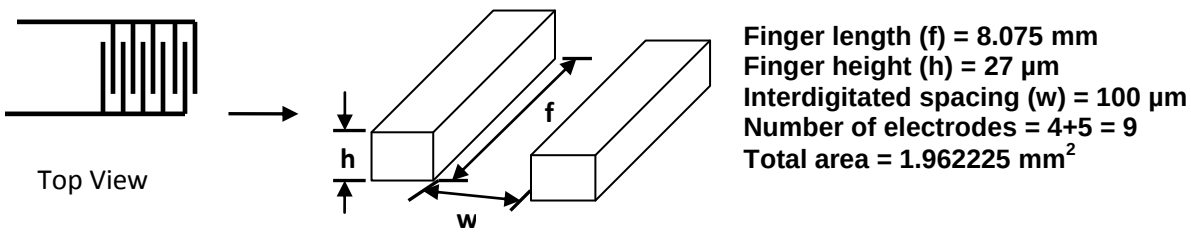

Figure 4.5 Schematic of interdigitated gold electrodes.

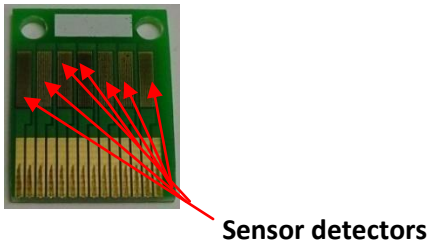

Figure 4.6 Custom built sensor chip showing 7 detectors.

4.6 Humidity Setup

The humidity of the various concentrations of CO_2 gases were increased from 20 to 80% relative humidity by bubbling through water. The controlled humidified analyte gases at room temperature (25±2ºC) were introduced steadily at a constant flow rate from the bubblers into the flow cell. The actual humidity of the analyte gas was monitored by a calibrated humidity sensor (Model HIH-4000, Honeywell Sensing and Control, Golden Valley, MN).

The HIH-4000 sensor contains a capacitive sensing die, set in thermoset polymers that interact with platinum electrodes. The HIH-4000 sensor has an integrated circuit which when supplied with an excitation voltage produces a DC

voltage output which is proportional to the relative humidity. The HIH-4000 sensor was connected to an Agilent data acquisition 37970A unit ((Agilent Technologies, Inc., Santa Clara, CA) through a screw terminal which supplied the excitation voltage. The calibration of HIH-4000 sensor was done against known concentrations of standardized KOH solutions of different concentrations. The display output from the data acquisition system was calibrated against the readings, with the slope and offset (Greenspan, 1977; Solomon, 1951).

The relationship between humidity level and ratio of flow rate passing through a bubbler containing water to the total flow rate is shown in Figure 4.7. For example, gas flow of 97 sccm of N_2 through bubbler by MFC1 and 103 sccm of N_2 from MFC9 into the mixing chamber will produce 70% r.h. at 25°C.

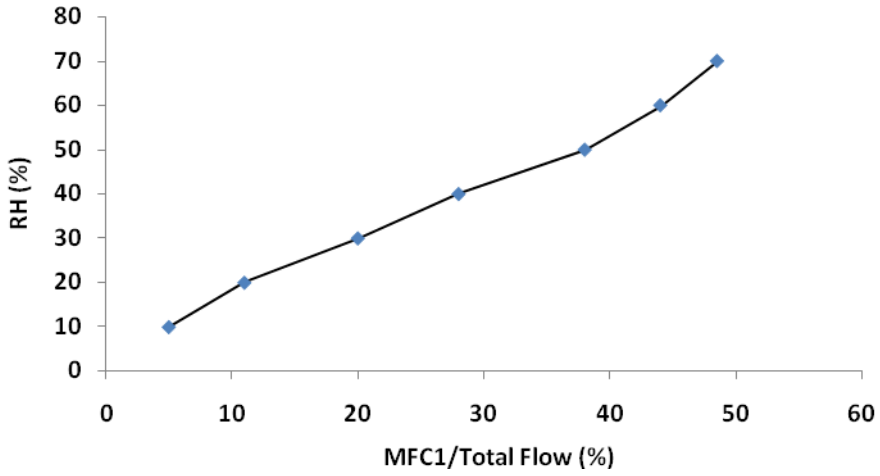

Figure 4.7 Relationship between humidity level and flowrate of nitrogen through MFC1 and MFC 9.

5. RESULTS AND DISCUSSION

5.1 Volatiles from Multiple Species

The GC-MS is composed of gas chromatograph and the mass spectrometer. The gas chromatograph utilizes a capillary column which depends on the column's dimensions such as length, diameter, film thickness as well as the phase properties. The working principle is based on the concept that the difference in the chemical properties between different molecules in a mixture will separate the molecules as the sample travels the length of the column. The molecules take different amounts of retention times to elute from the gas chromatograph. The different elution and retention times allows the mass spectrometer downstream to capture, ionize, accelerate, deflect, and detect the ionized molecules separately. The mass spectrometer accelerates the molecules by breaking each molecule into ionized fragments and detects these fragments using their mass to charge ratio. GC-MS analysis of the pure wheat samples at 16.5 and 19% m.c. stored for six weeks had octanol and nonanal volatile metabolites. This may be due to the formation of fungi in the wheat bulk. Fungal infection was also observed visibly on grain kernel surfaces from these samples. Hence, these samples were not used for control samples for background subtraction and only 14% moisture content samples were used as controls.

The chewing of wheat kernels by insects and chemical reactions caused by fungal infection on the kernel surface inside the grain bulk can alter the flavor and nutritive value and produce a range of volatiles (Magan and Evans, 2000).

This study emphasized on identifying volatile metabolites produced by wheat bulks infested by a co-occurrence of species. Microbial analysis enables characterization of the microorganism profile (type and the amount of fungi) and also can quantify the concentration of volatile metabolites produced by fungi and insects. However these analyses are time-consuming and require an experienced microbiologist to correlate fungi concentration with odor. Methodology used to elute volatiles from infested grain did not allow to accurately quantifying the concentration of volatile metabolites produced by fungi and insect species inside wheat bulks. Quantification is possible by calculating the peak area of each volatile in the GC-MS spectra and by comparing with the peak area of a standard for relative percent calculations but converting it to per unit mass of grain or per unit insect is not easy. Also, it is not possible that each grain kernel will be similarly infected by fungi. Therefore, quantification was not done and only the presence of compounds was recorded.

Table 5.1 shows the compounds identified by the GC-MS analysis of the infested samples. Volatile metabolites produced by wheat bulk infested by *Aspergillus niger*, *Penicillium* spp., rusty grain beetle and red flour beetle alone correlate with the published results (Sinha et al., 1988; Loschiavo et al., 1986; Seitz and Ram, 2000). Infestation of wheat bulk by *A. niger* and red flour beetle, *A. niger* and rusty grain beetle produced only one compound methyl isobutyl

ketone. Wheat bulks infested by *Penicillium* spp. and rusty grain beetle produced methyl isobutyl ketone and 2,3-dimethyl-2-butanol. A combination of *Penicillium* spp. and red flour beetle produced methyl isobutyl ketone and 1,4-dimethoxybenzene metabolites. Moisture content had no significant effect on the identity of volatile metabolites as wheat of all three moisture contents produced the same compounds except for the wheat bulk infested with *Aspergillus niger*.

Table 5.1 Volatiles obtained from Canada Western Red Spring wheat infested by insects and fungi.

Moisture content	Infestation type	Volatile
14%	*Aspergillus niger*	1-octanol; nonanal; 2-ethyl-2-hexenal
16.5%	*Aspergillus niger*	1-octanol; nonanal; 2-ethyl-2-Hexenal
19%	*Aspergillus niger*	1-octanol; naphthalene; 2-ethyl-2-hexenal; 1,2,3-trimethyl-benzene
14%	*Penicillium* spp.	2-methyl-1-butanol; 1-octen-3-ol; 3-octanone
16.5%	*Penicillium* spp.	2-methyl-1-butanol; 1-octen-3-ol; 3-octanone
19%	*Penicillium* spp.	2-methyl-1-butanol; 1-octen-3-ol; 3-octanone
14%	Rusty grain beetle	2-methyl-3-phenyl-propanal; 3-dodecen-11-olide
16.5%	Rusty grain beetle	2-methyl-3-phenyl-propanal; 3-dodecen-11-olide
19%	Rusty grain beetle	2-methyl-3-phenyl-Propanal, 3-dodecen-11-olide

14%	Red flour beetle	2-ethyl-1,4-dimethoxybenzene; 1,4-dimethoxybenzene; 1-pentadecene
16.5%	Red flour beetle	2-ethyl-1,4-dimethoxybenzene; 1,4-dimethoxybenzene, 1-pentadecene
19%	Red flour beetle	2-ethyl-1,4-dimethoxybenzene; 1,4-dimethoxybenzene; 1-pentadecene
14%	*Aspergillus niger* + *Penicillium* spp.	1-(4-ethylphenyl)-ethanone; Methyl ester dodecanoic acid; (2-methylpropyl)- Benzene; 2,4-Pentanedione
16.5%	*Aspergillus niger* + *Penicillium* spp.	1-(4-ethylphenyl)-ethanone; Methyl ester dodecanoic acid; (2-methylpropyl)- benzene
19%	*Aspergillus niger* + *Penicillium* spp.	1-(4-ethylphenyl)-ethanone; Methyl ester dodecanoic acid; (2-methylpropyl)- benzene
14%	Rusty grain beetle + red flour beetle	Methyl isobutyl ketone; 2,3,5,6-tetramethyl-phenol
16.5%	Rusty grain beetle + red flour beetle	Methyl isobutyl ketone; 2,3,5,6-tetramethyl-phenol
19%	Rusty grain beetle + red flour beetle	Methyl isobutyl ketone; 2,3,5,6-tetramethyl-phenol
14%	*Aspergillus niger* + rusty grain beetle	Methyl isobutyl ketone
16.5%	*Aspergillus niger* + rusty grain beetle	Methyl isobutyl ketone

19%	*Aspergillus niger* + rusty grain beetle	Methyl isobutyl ketone
14%	*Aspergillus niger* + red flour beetle	Methyl isobutyl ketone
16.5%	*Aspergillus niger* + red flour beetle	Methyl isobutyl ketone
19%	*Aspergillus niger* + red flour beetle	Methyl isobutyl ketone
14%	*Penicillium* spp. + rusty grain beetle	Methyl isobutyl ketone; 2,3-dimethyl-2-butanol
16. 5%	*Penicillium* spp. + rusty grain beetle	Methyl isobutyl ketone; 2,3-dimethyl-2-butanol
19%	*Penicillium* spp. + rusty grain beetle	Methyl isobutyl ketone; 2,3-dimethyl-2-butanol
14%	*Penicillium* spp. + red flour beetle	Methyl isobutyl ketone; 1,4-dimethoxybenzene
16. 5%	*Penicillium* spp. + red flour beetle	Methyl isobutyl ketone; 1,4-dimethoxybenzene
19%	*Penicillium* spp. + red flour beetle	Methyl isobutyl ketone; 1,4-dimethoxybenzene

5.2 Sensor Principle

The sensing mechanism is based on the interconversion between conducting emeraldine salt form and the insulating emeraldine base form of poly aniline and PABA through protonation and deprotonation.

When the analyte (gaseous CO_2) permeates through the gas permeable membrane, CO_2 reacts with water from PVA to create a bicarbonate ion (HCO_3^-) and a proton, which protonates the poly aniline. When the CO_2 diffuses through the gas-permeable membrane, the following equilibria are sequentially established (Jensen and Rechnitz, 1979).

$$CO_2\ (aq) + \mathrm{H_2}0 \rightleftarrows\ H_2CO_3 \qquad (2)$$

$$H_2CO_3 \rightleftarrows H^+ + HCO_3^- \qquad (3)$$

$$HCO_3^- \rightleftarrows H^+ + CO_3^{2-} \qquad (4)$$

As the CO_2 partial pressure increases, the conductivity increases due to increase in the amount of protonation. This changes the pH of the internal electrolyte. The change in pH is related to the potential of the PABA thin film through the Nernst equation (Eq 5). The potential changes linearly with the pH and thereby the concentration of the analyte can be measured.

$$E = E^\circ - \frac{0.0591}{z}\ log\ \frac{a_{Red}}{a_{Ox}} \qquad (5)$$

where z is the number of moles of the electrons involved in the reaction, a is the chemical activity for the relevant species, Red is reduction and Ox is oxidation.

Nernst equation relates the potential of electrochemical cell (or sensing assembly) as a function of concentration of ions in the reaction. Figure 5.1 illustrates the potentiometric response of PABA to changes in H^+ ion concentration revealing a Nernstian response slope of m = -59 mV pH^{-1} for buffer solutions from pH 1 to 8.

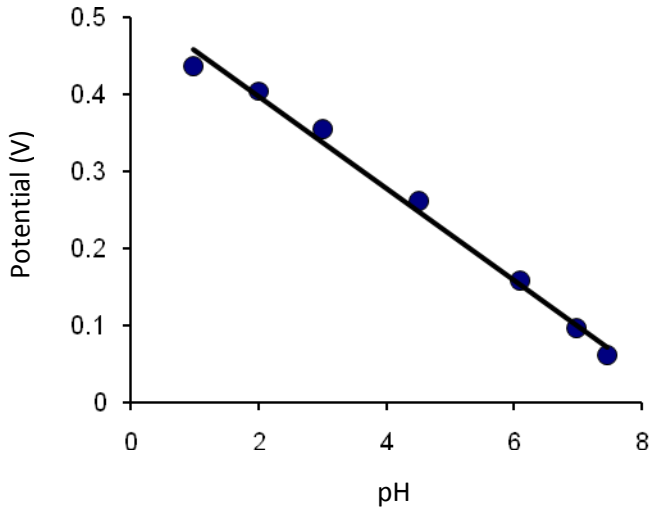

Figure 5.1 Open-circuit potential response of PABA film with varying pH of solution.

Sensing measurements were done at different potentials using amperometry at the working electrode. For all the amperometric measurements, a constant

potential of 0.01 V (optimized potential) on the sensor was applied which facilitated a wider linear range, steady-state, response current output.

Figure 5.2 shows typical response behaviour of the PABA film to change in pH at an excitation voltage of 0.2 V which was determined as an optimum voltage during preliminary experiments at 0.1 to 0.5 V. A 3 µL PABA solution deposited and dried on the gold IDA was characterized for its sensitivity to change in pH in 0.1 M KCl and sodium phosphate buffer solution. The change in pH of the buffer solution was achieved by adding 1 M H_2SO_4. The PABA showed linear response in the near neutral pH range of 4-7, and therefore, was selected for use as sensing material for constructing a CO_2 sensor. The results of this experiment confirmed the desired pH response properties of PABA thin film such as stability, response time and linear range.

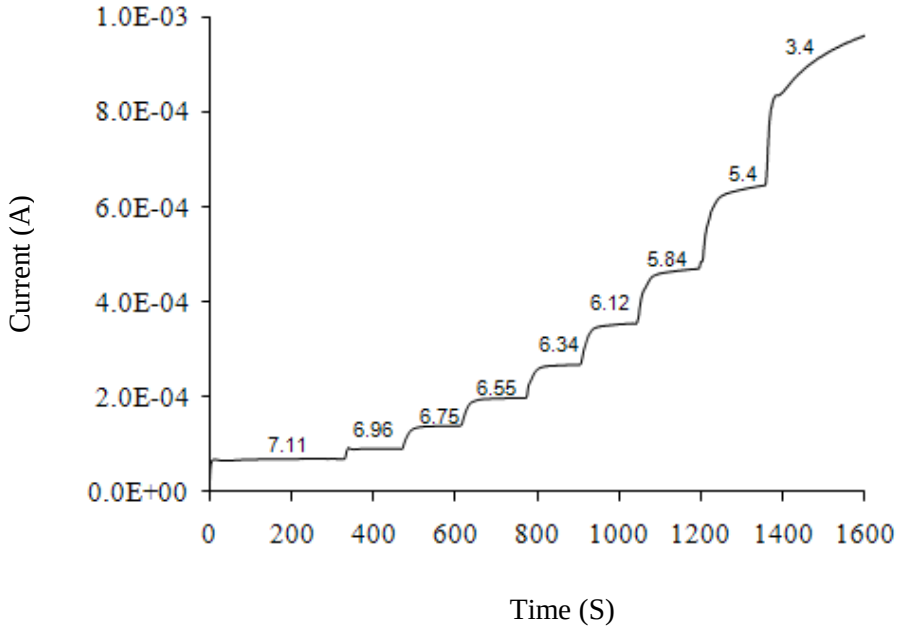

Figure 5.2 Current measurement of PABA film at 0.2 V as a function of pH of solution.

The sensors were placed in the Teflon test chamber and were exposed, alternately, to clean dry background air and air containing analyte. The sensor exposures alternated between 5 min of clean background air and 5 min of different analyte concentrations for each analyte concentration. Baseline resistance for each sensor was established by flowing background air (air containing 380 ppm of CO_2) and at 0% humidity prior to various nitrogen and CO_2 exposure levels. Sensor data were recorded as resistance versus time and the events such as an exposure to various CO_2 levels or a change in humidity or temperature were analyzed as normalized changes in resistance ($\Delta R_m/R_b$).

$$\frac{\Delta R_m}{R_m} = \frac{(R_m - R_b)}{R_b} \qquad (6)$$

R_m = sensor resistance at the plateau of the response

R_b = resistance prior to the event

The displayed graph data were processed using background determination as Rb prior to an exposure of analyte to correct for baseline drift.

The PABA film thickness was calculated from the volume of the solution (3 µL) divided by the area of the electrode (0.0609 cm^2) as 492 microns. This calculation of average film thickness is prone to errors considering the coulombic efficiency, sticking coefficient and substrate tilt angle.

5.3 Performance of PABA Sensor without Electrolyte

For functional feasibility, the sensor industry prefers solid electrolyte over liquid electrolyte to maintain compactness of sensor cells considering the size of packaging components, leakage, and drying up of liquid electrolyte under high humidity/temperature conditions. Among the solid electrolyte polymers known, Nafion is the best in terms of conductivity and chemical resistance properties (Viswanathan et al., 2007; Hu et al., 2008). Nafion functions as an acid catalyst due to strongly acidic properties of the sulfonic acid group, and also as an ion exchange resin. The sulfonic acid groups in Nafion have a very high water-of-hydration. Interconnections between the sulfonic acid groups lead to rapid transfer of water through the Nafion. Nafion has been widely used as a proton exchange membrane in polymer electrode fuel cell applications.

The sensor electrodes prepared with only PABA and without Nafion were exposed to different concentrations of CO_2 at various humidity levels.

No response was observed from the electrodes below 40% r.h. For protonation to occur to facilitate the exchange of ions upon exposing to analyte, PABA requires water molecules. So, at higher humidity levels above 40% RH, the PABA was able to respond to analyte concentrations (Figure 5.3) and this could be due to the absorption of water molecules from air. The resistivity was seen to increase slightly from 40% to 70% RH. The baseline resistance of the sensor during background airflow increased from 4300 ohms at 40% RH to 5750 ohms at 70% RH. The sensors exhibited quick response for changing humidity

and the response and recovery times were of the order of few seconds. The variation in the resistance parameters was nearly linear and was repeatable. The sensor electrodes show a saturation effect at 2455 ppm.

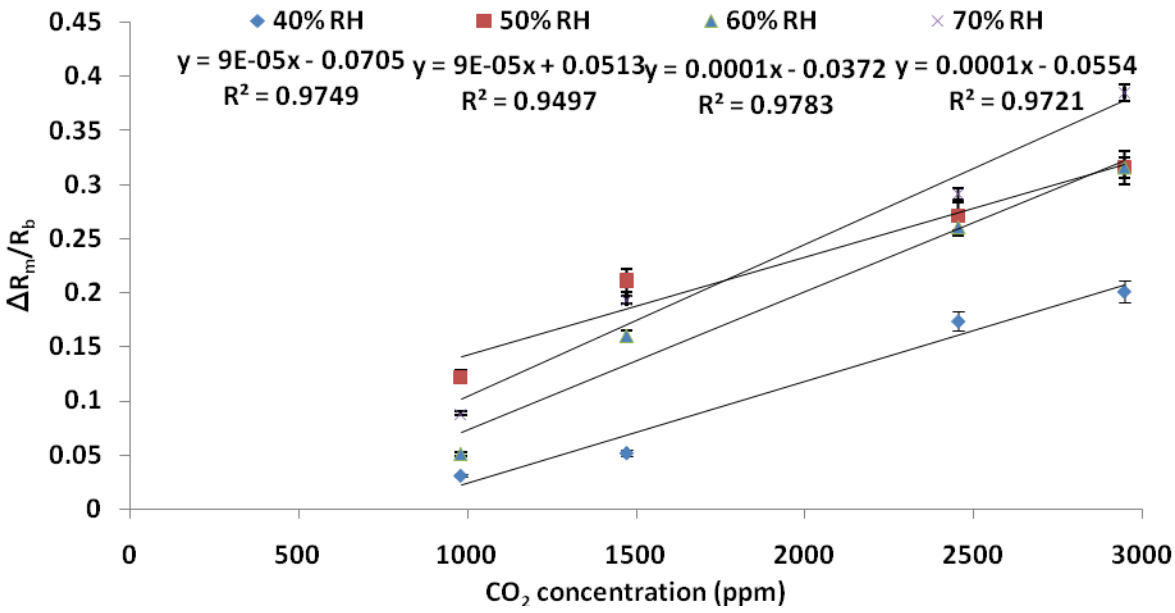

Figure 5.3 Response of PABA sensor electrodes (without electrolyte) to various concentrations of CO_2 at different humidity levels and at 25° C for 5 replicates.

5.4 Effect of Humidity

The results of the relationship between resistance and CO_2 concentration for the PABA-Nafion sensor under various humidity levels are shown in Figure 5.4.

The humidity has less pronounced effect on the performance of the PABA Nafion sensor. It has been reported (Skotheim et al., 1998) that the conductivity of conducting polymers increases when the film absorbs the moisture. The

resistance value of PABA decreased with humidity level due to the possibility of proton exchange between the water molecules and the protonated and the unprotonated forms of PABA.

PABA-Nafion sensor showed two step sensing response to humidity levels. The resistance value of the sensor electrodes decreased when RH increased from 20 to 50% indicating that the water molecules might have been absorbed by the PABA film. The charge transfer process of conducting species with water molecules resulted into the decrease in the resistance value. The resistance values of the sensor increased when RH increased from 50% to 70%. The mechanism of charge transfer process may be different for the humidity levels between 50 to 70% RH. The deviation in the linearity could be attributed to the size of the pores of polymer. Similar deviation in the linearity behaviour was observed by Parvatikar et al. (2006) in a PANI/WO_3 composite sensor when exposed to humidity levels between 20 to 90% RH. The polymer might swell due to water absorption and there may be breakdown or increase in contact between the dispersed conductive nano particles affecting the resistance value with the change in humidity. The polymer backbone might swell due to the change in humidity and the pathways inside the film might be saturated with water leading to change in the diffusion rate of gases into the polymer matrix. As the humidity increases from 20% to 50% RH, there may be more hydrogen carbonate ions and protons produced on the PABA film, thus lowering the resistance of the film. Above 50% RH level, the pores might be saturated causing a change in diffusion pathways. The variation in the resistance parameter was curvi-linear and

repeatable. The film's response to change in analyte concentrations at various humidity levels was very stable until 70% RH and becomes noisy above 70% RH. At humidity levels above 70% RH, the sensors might still perform well when provided with a rugged membrane protection and a proper sensor packaging. Irrespective of the change in resistance values at different humidity levels, all the PABA-Nafion sensors responded to various levels of CO_2 concentrations up to 2455 ppm.

The variations in the resistivity as a function of relative humidity value for the PABA sensor is depicted in the Figure 5.5.

The percentage sensitivity as a response to humidity is defined as:

$$S = \left[\frac{(RH2 - RH1)}{RH1}\right] \times 100 \quad (7)$$

where RH2 is the resistivity of the PABA sensor for humidity at level 2, and RH1 the resistivity of the PABA sensor for humidity at level 1.

PABA-Nafion sensor's sensitivity shows two step responses at various humidity levels. The behavior of the sensors is almost linear from 20 to 40% RH (Figure 5.4). A saturation effect is observed between 40 to 50% RH and the sensitivity of the sensor decreases above 60% RH. The conductivity of PABA increases when the sensing material absorbs the moisture. With the adsorption of water molecules at increasing humidity levels, the resistance decreases from 20 to 40% RH. Partial charge transfer process of conducting species with water

molecules might result into the decrease in the resistivity. This mechanism might be different at higher humidity levels.

The decrease in the resistivity value or the increase in conductivity could also be attributed to the geometry of the polymer and the charge transfer across the polymer chains. The sensor electrodes display a saturation effect above 2455 ppm of CO_2. The sensor's working principle depends on the extraction of ions and electrons and due to the change in protonation state from the PABA film. With larger porous structure, the PABA film will provide a large reaction surface and inner space for the electrolyte penetration into the film. So, this might shorten the diffusion pathways for the counter ions and lead to quicker response time. Changing the morphology of films by creating a higher surface area through nanorods or nanofiber structures in the poly aniline film might enhance the sensitivity and response time of the sensor (Virji et al., 2004).

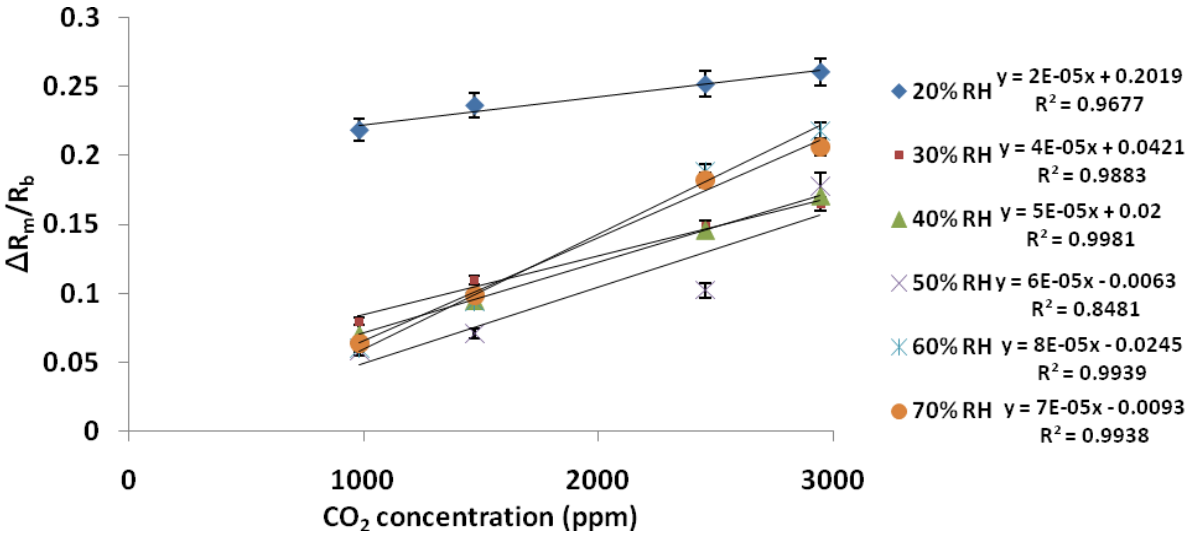

Figure 5.4 Variation of resistance with change in relative humidity (%) for PABA-Nafion sensor at 25°C for 7 replicates.

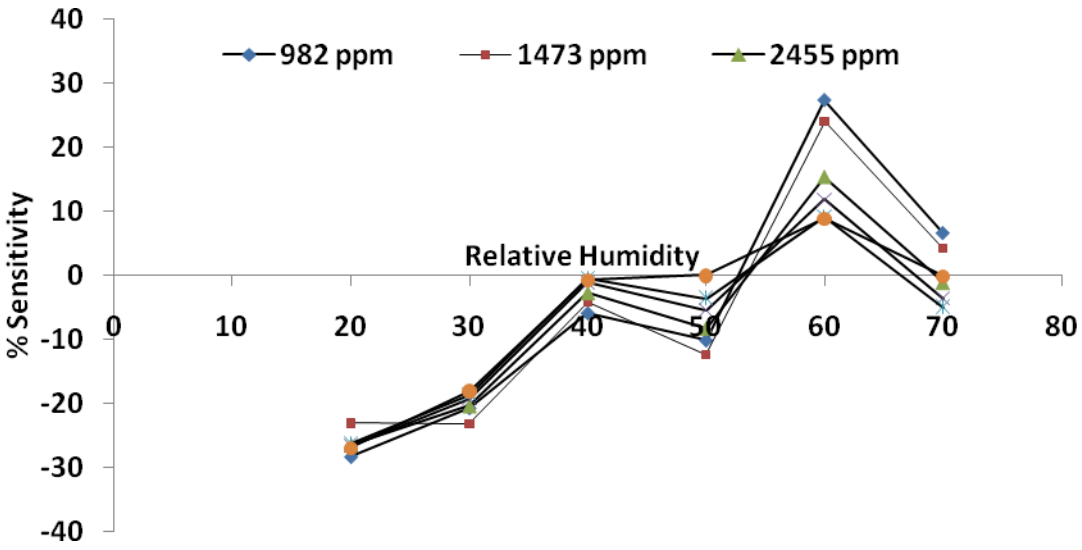

Figure 5.5 Variation of sensitivity with change in relative humidity (%) for PABA-Nafion sensor at 25°C for 7 replicates.

5.5 Effect of Temperature

The influence of temperature on the performance of the constructed sensors was evaluated by allowing the analyte gas to pass through a copper coil immersed in heated water bath circulator (Model 12108-20 Cole-Parmer Instrument Company, Vernon Hills, IL). The temperature range was maintained from 25°C to 55°C. The sensor chip was also tested at various CO_2 levels after storing the chip at -25°C for 48 h and then at the room temperature for about 2 h before placing it in the testing chamber at 25°C. The temperature of the analyte gas inside the testing chamber was monitored using a temperature sensor (Model 44034 Omega Precision Thermistor, Omega Engineering Inc, Stamford, CT).

For the PABA-Nafion sensor, the resistance value decreased from 6000 to 1044 ohms when the temperature increased from 25°C to 55°C when exposed to 2455 ppm CO_2. Experiments were conducted by changing the order of heating the CO_2 gas flow and similar trend was observed indicating that the phenomenon is reversible irrespective of the temperature order. The decrease in the resistance value upon increase in temperature (Figure 5.6) may be due to the loss of protonation and expulsion of water molecules from the polymer composite. In terms of thermal stability, the influence of the acid used for the protonation of PANI is more than the poly aniline backbone itself, because poly aniline has the ability to sustain exposure to an elevated temperature of 173°C without decisive damage (Prokes and Stejskal, 2004). Thermogravimetric analysis of PABA by Yu et al. (2005) proves that the thermal stability of PABA is greater than that of other self-doped forms of poly aniline. When exposed to above 400°C, poly aniline experiences complete decomposition of the backbone, while PABA remains intact and possesses a high level of conductivity. The increase in resistance value with exposure to -25°C may be explained by the change in the morphology of the film and the restriction of the transportation of charge carriers.

The percentage sensitivity as a response to temperature is defined as:

$$S = [(T2 - T1)/T1]\,100 \qquad (8)$$

where T2 is the resistivity of the PABA sensor for temperature level 2, and T1 is the resistivity of the PABA sensor for temperature at level 1.

PABA-Nafion sensor's sensitivity shows saturated response to analyte between 25°C to 45°C (Figure 5.7). The sensitivity of the sensor decreases above 45°C. The conductivity of PABA decreases with loss of moisture from the sensing material. The chain alignment of the polymer and the charge transfer between the polymer chains and dopants might be influenced by thermal curing leading to decrease in resistance value. When poly aniline is serving as a donor, the thermal excitation of electrons in poly aniline facilitates the charge transfer. However, if poly aniline assumes the role of an acceptor, the charge transfer becomes less efficient at higher temperatures (Li et al., 2004). In our study, the charge transfer complex formed between poly aniline donor and carbon dioxide acceptor molecules might explain the difference in sensitivity level of the sensor towards carbon dioxide at different temperatures. The boronic acid dopant may act as tunneling bridges for charge mobility along the polymer backbone as well as donor and acceptor sites for the target carbon dioxide molecules. The sensor did not respond to various CO_2 concentrations and the response became noisy above 55°C. To assess the influence of temperature, experiments were conducted at 50% RH for measurements at 25°C. As the temperature increased from 25 to 55°C, the water molecules in the air might be reduced to a greater extent. Further investigations are needed to evaluate the performance of PABA-Nafion sensor at various temperatures and at higher humidity levels.

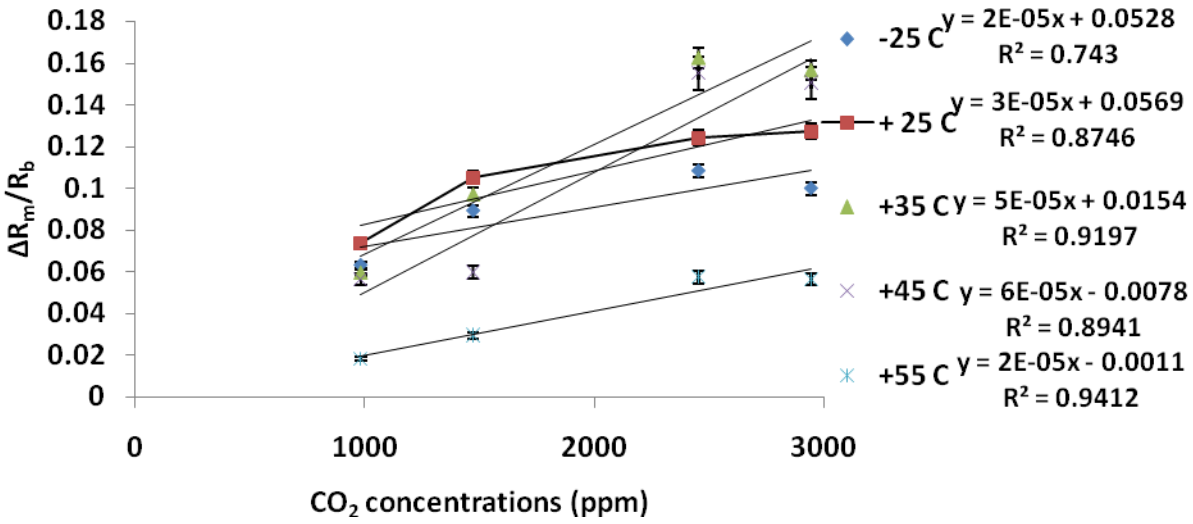

Figure 5.6 Variation of resistance with change in temperature (°C) for PABA-Nafion sensor at 50% RH level for 7 replicates.

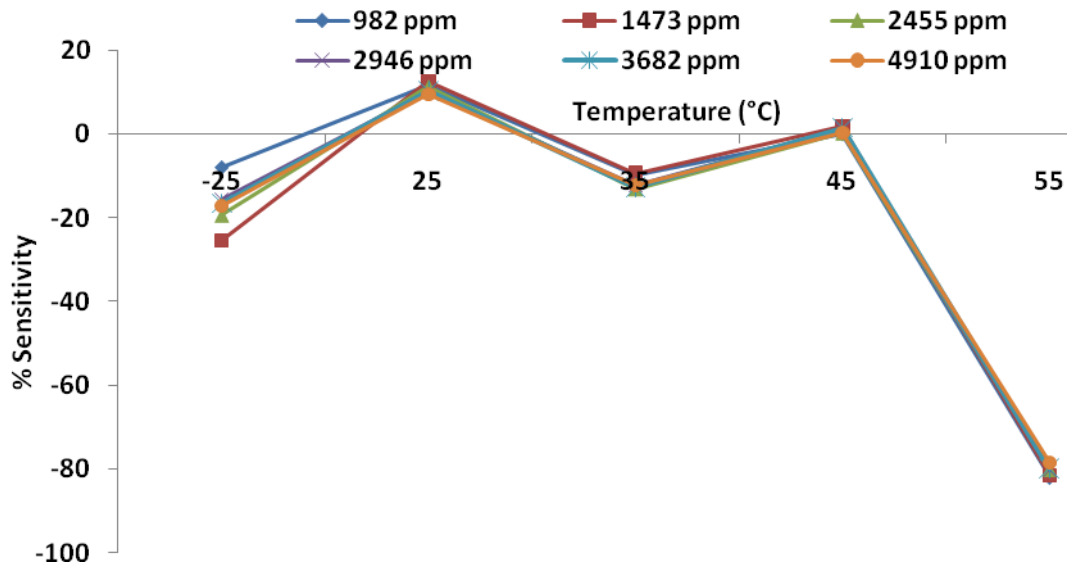

Figure 5.7 Variation of sensitivity with change in temperature (°C) for PABA-Nafion sensor at 50% RH level for 7 replicates.

5.6 Repeatability and Reproducibility

Sensor repeatability refers to the successive runs made using a single sensor to evaluate discrepancies in its response. Sensor reproducibility refers to the sensor variations in response between individual chips of a batch of similarly constructed sensors. The repeatability of the sensor was studied by using the same sensor to repeatedly (five times) measure the response to different CO_2 concentrations (Figure 5.8). At the same time, the reproducibility of the sensor was studied by using five similarly constructed sensors to measure the response at various CO_2 gas levels (Figure 5.9).

In the reproducibility study, the same response trend was observed for all of the sensors on the same chip. Each sensor chip has seven sensors and the response of the sensors is shown in Figure 5.8. The response of the sensors was not stabilized initially and over the course of time, it became stabilized. The relative standard deviation (R.S.D.) for reproducibility of the sensor was 11%. Variation in the response of the sensor could be due to the construction variation and operational variation. The sensitivity got better with time/exposure as trial 4 and trial 5 responses are nearly overlapping. The same trend was observed for all sensor electrodes in different chips (data not shown).

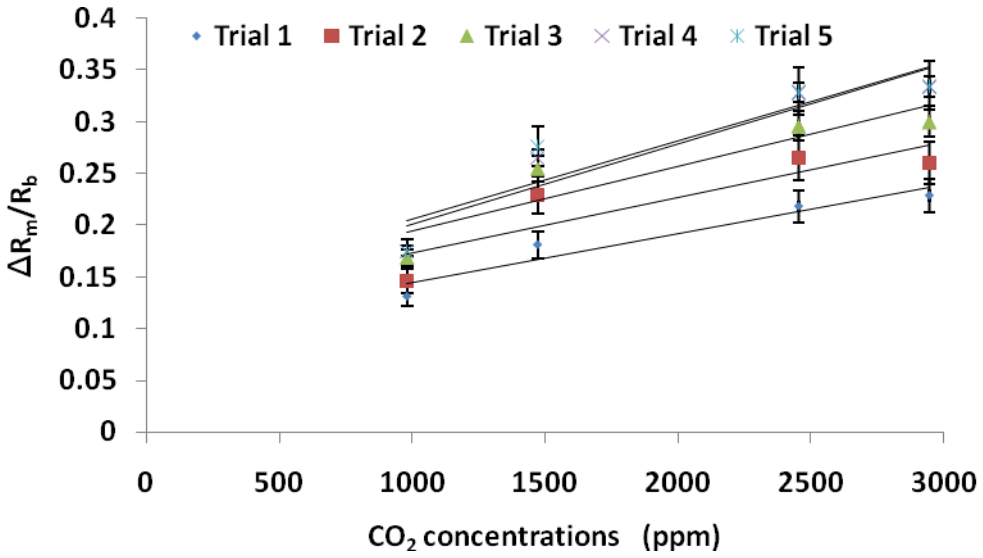

Figure 5.8 Response of PABA-Nafion Sensor Chip #64 (5 trials, same electrode) to various concentrations of CO_2 at 40% RH and at 25° C.

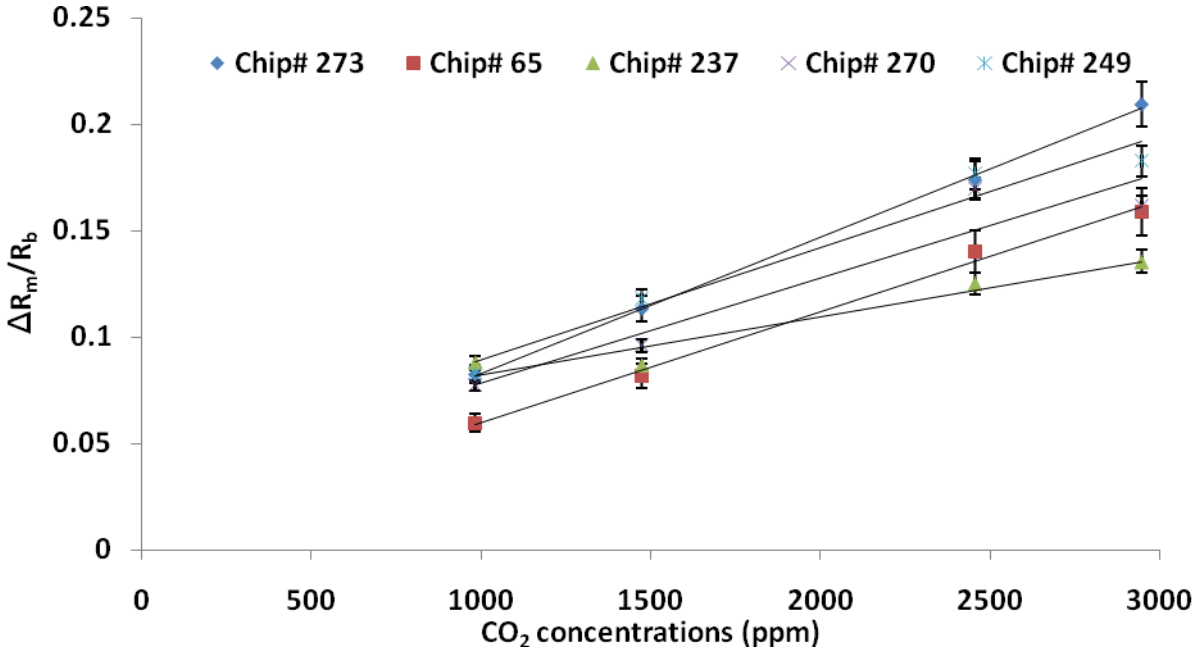

Figure 5.9 Response of 5 different similarly constructed PABA-Nafion sensors to various concentrations of CO_2 at 40% RH and at 25° C.

To study the human-error prone fabrication procedures and to observe the replication on reproducibility, sensors were prepared by another researcher (operator 2) with similar construction parameters. Operator 2 prepared the sensor electrodes using the physical dispersion process and tested the same under various concentrations of CO_2 at 50% RH.

Variation between the sensor responses prepared by 2 different researchers could be due to the operational and constructional parameter variations. The relative standard deviation was 6% and 7% for the operator 1 and operator 2, respectively, which is less than 11%, the reproducibility R.S.D of the sensor prepared by user 1 (Figure 5.10). Hence, the human-error prone fabrication errors are not significant. Performance wise, sensors prepared by user 1 and user 2 behaved in a similar fashion as the saturation effect was observed above 2455 ppm of CO_2.

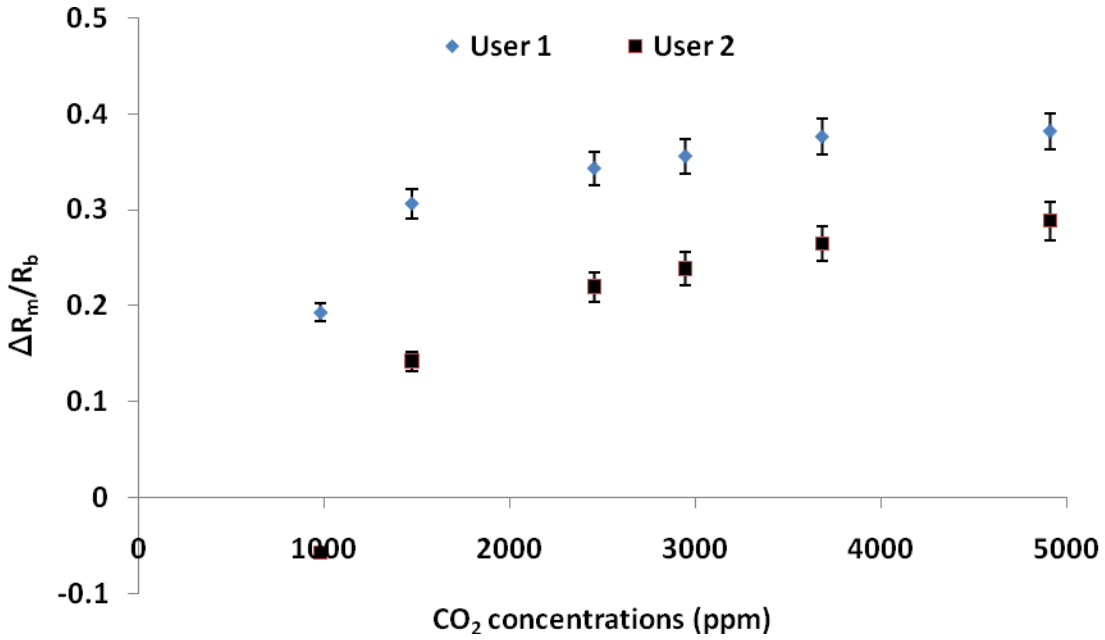

Figure 5.10 Response of similarly constructed PABA-Nafion sensor chips by 2 different users to various concentrations of CO_2 at 40% RH and at 25°C (Means of 5 replicates for each sensor).

5.7 Dynamic Characteristics

Sensitivity, linearity, accuracy, drift and hysteresis properties have transient effects that are settled to their steady state and are the static characteristics of sensor. The experimental results on the effect of humidity and temperature indicate that the response of the PABA-Nafion sensor to various levels of CO_2 is linear up to 2455 ppm and above that a saturation effect is observed. Prior to actual measurements, the sensor was exposed for 20 min in the background gas flow to achieve stabilized response and to reduce associated drift. The repeatability and reproducibility experiments results show that the PABA-Nafion

sensor is accurate with higher sensitivity. A sensor's sensitivity indicates how much the sensor's output changes upon exposure to analyte. Drying the sensor electrodes after material deposition over 30 min reduced the drift to a large extent.

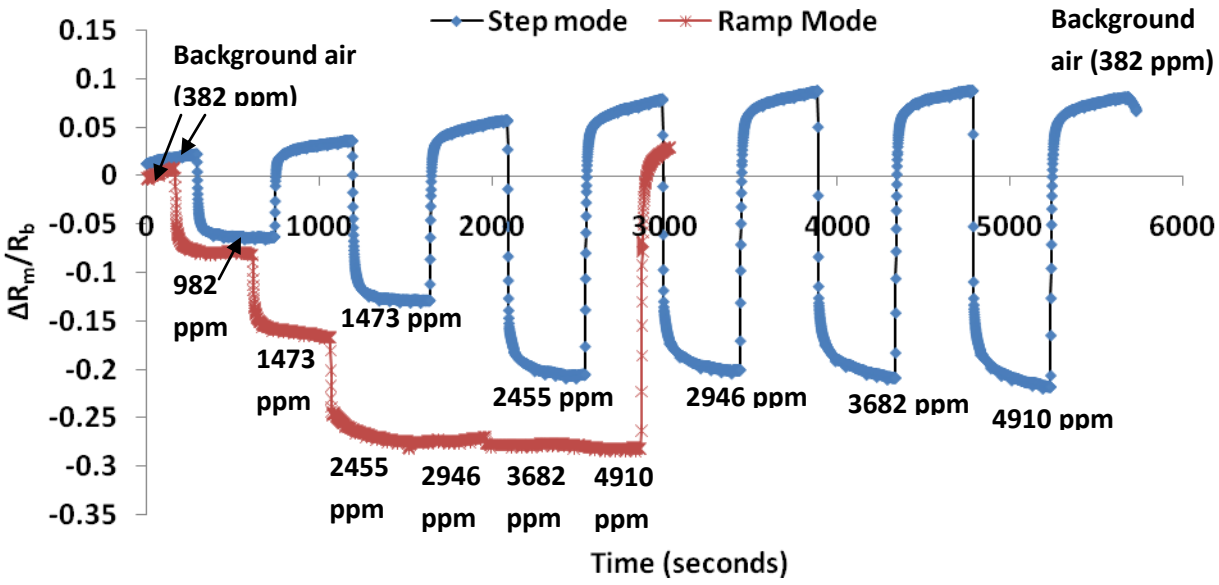

Figure 5.11 Response of the PABA-Nafion sensor operated in step and ramp mode to various concentrations of CO_2 and subsequent exposure to background air at 40% RH and at 25°C.

The dynamic characteristics of a sensor are determined by analyzing the response of the sensor to variable input of analyte (CO_2) concentrations such as step mode, ramp mode (Figure 5.11) and random measurement (Figure 5.12). Characterization of the PABA-Nafion sensor's dynamic response was evaluated by comparing the step mode and ramp mode measurement. The ramp mode response curve shows that the PABA-Nafion sensors did not respond to CO_2

levels above 2455 ppm. The step or pulsed mode measurement shows that the response curve was reversible upon exposure to background gas.

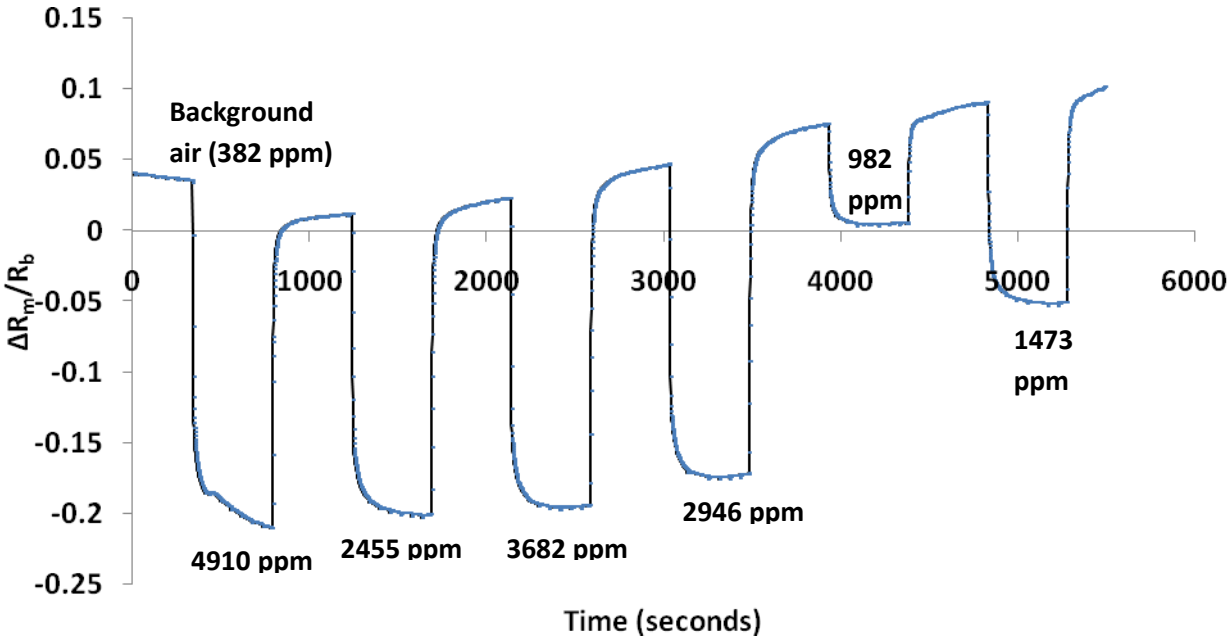

Figure 5.12 Response of the PABA-Nafion sensor operated in random mode to various concentrations of CO_2 and subsequent exposure to background air at 40% RH and at 25°C.

5.8 Evaluation of Gas Permeable Membrane

The gas permeable membranes play an important role in limiting the diffusion rate of CO_2 as well as selectively pass the analyte into the electrolyte reservoir. By selecting appropriate gas permeable membranes with different pore size and thickness, the sensitivity and (or) the linear range of the sensor can be optimized to certain extent. The membranes act as a protecting cover for the electrolyte

and the sensing material in the sensing reservoir on the electrode arrays. The PTFE membrane is highly selective to CO_2 and does not allow other gas molecules to pass through hence aiding in reducing the cross-sensitivity effect of the sensor (Figure 5.13).

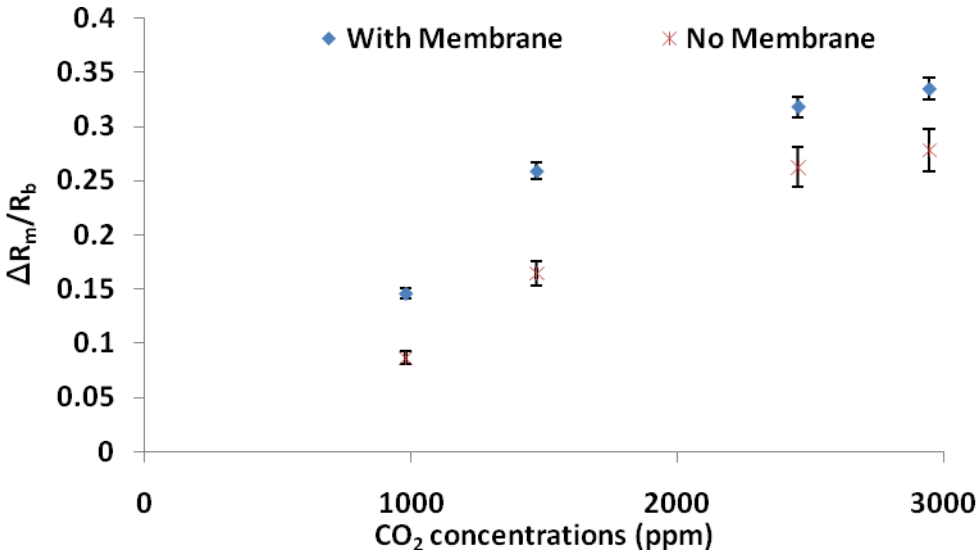

Figure 5.13 Response of the PABA sensor with and without selective gas permeable PTFE membrane to various concentrations of CO_2 and subsequent exposure to background air at 40% RH and at 25°C for 5 replicates.

5.9 Effect of Cross Sensitivity

For efficient functioning of sensors, there is a need to find out whether the sensor is interfered by other gases in addition to target analyte gas. The dc resistance values decreased with increasing CO_2 concentration indicating an increase of conductivity due to CO_2 concentration levels. But upon random

exposure of 1% (percent of vapour pressure) of methanol, acetone and 1-propanol (representative of compounds expected in stored grain) in air for 3 min, followed by various levels of CO_2 did not change the resistivity of the sensor. The PABA-Nafion sensor works on the principle of pH change and CO_2 being acidic reacts with the electrolyte to induce ionic exchange resulting in decreased resistivity. The gas permeable membrane is selective to CO_2 and allows only CO_2 molecules to pass through. Hence there was no response (Figure 5.14) due to alcohols and ketones in air.

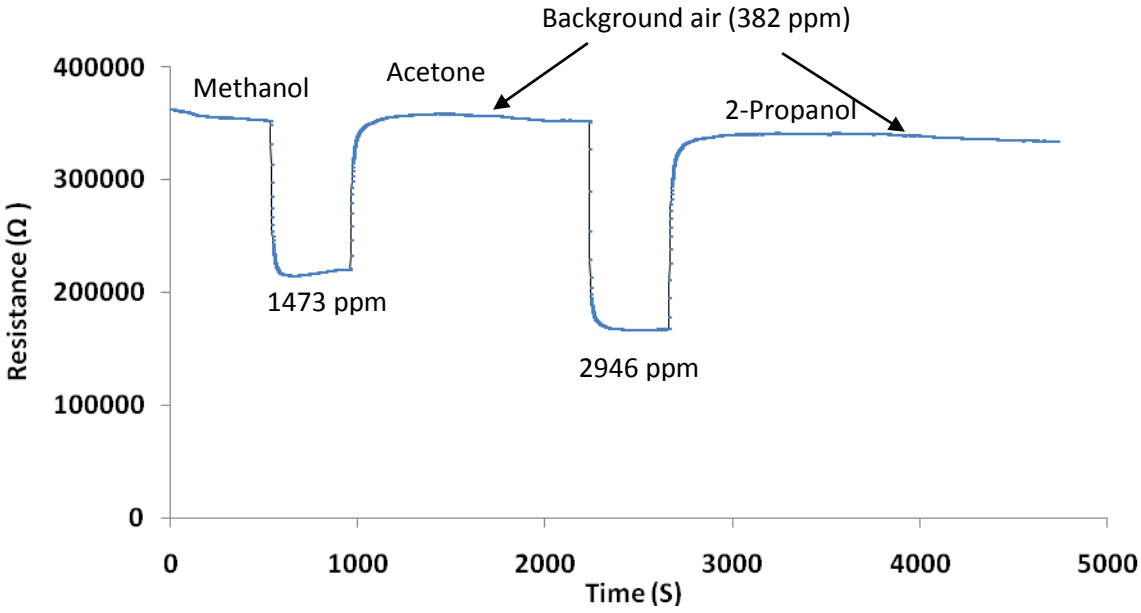

Figure 5.14 Response of the PABA sensor with selective gas permeable PTFE membrane to CO_2, methanol, acetone and 2-propanol analytes of 1% in air at 40% RH and at 25°C.

5.10 Influence of PVA Electrolyte

Similar to Nafion, Poly vinyl alcohol (PVA) is highly hydrophilic and capable of absorbing and retaining large amounts of water molecules from the atmospheric air. PABA sensors prepared with PVA electrolyte were tested under various concentrations of CO_2 in air. The sensor's response was similar to PABA-Nafion and a saturation curve was observed when exposed to above 2455 ppm of CO_2 gas (Figure 5.15). As the concentration of the CO_2 increases, the pH changes from neutral to acidic, which causes an increase in the conductivity of proton and thereby reducing the resistance of the flowing current in the film. The PVA sensor exhibited severe drift in comparison with PABA-Nafion sensor. But PVA sensor exhibited similar reversibility characteristics in sensing the CO_2 analyte in comparison with PABA sensor.

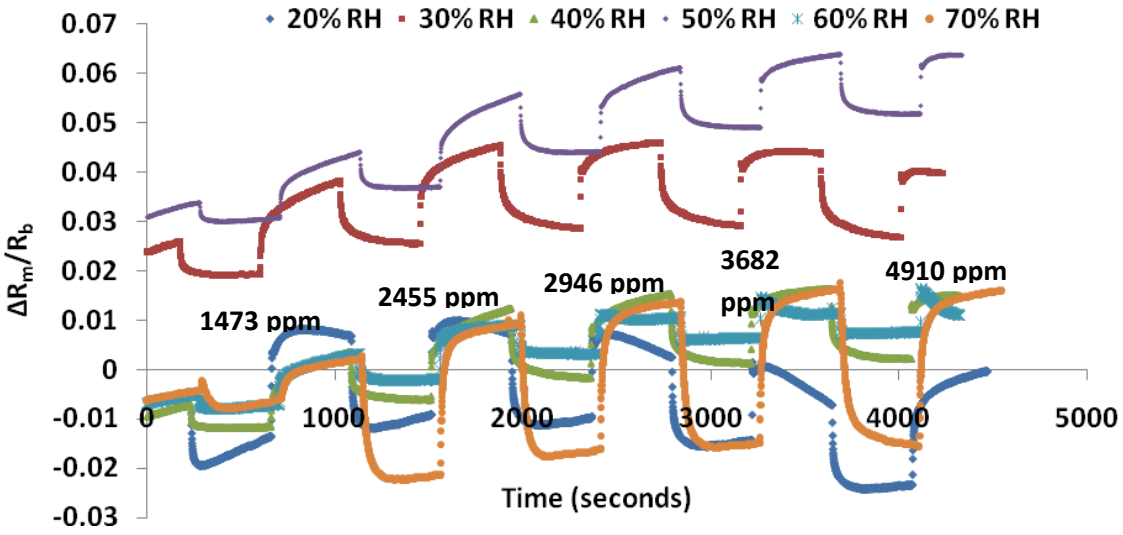

Figure 5.15 Response of PABA sensor with PVA hydrogel electrolyte to various concentrations of carbon dioxide at 25°C.

5.11 Results of Experiments to Increase Sensor Detection Range

Tailoring the pH response range of PABA sensor was attempted by using KCl as a dopant. It was hypothesized that chloride anions from KCl will exchange out the phospate from PABA resulting in the dedoping of PABA and thereby inducing the ionic conductivity. This might help to increase the detection range of the sensor and hence the PABA-Nafion sensor would be able to measure above 2455 ppm levels of CO_2. To increase the sensor's detection range, 2 µL of PABA deposited on sensor electrodes and dried for 20 min were immersed in 20 ml of 1 M, 0.5 M, 0.1 M, 0.01 M concentrations of KCl solutions and their resistance was monitored until the resistance data stabilized. This was done to ensure that the KCl is exchanging out the phosphate. The sensor electrodes were removed from the KCl solution and dried for 30 min and a 2 µL nafion was deposited on the top of the dried PABA phosphate exchanged out material. After drying for 30 min, the electrodes were tested under different concentrations of CO_2 levels. The results did not show increase in the detection range and the response curves were similar with same detection window (stabilization after 2455 ppm) to the without treatment PABA-Nafion sensors.

To achieve more controlled doping of KCl with phosphoric acid in PABA, five different solutions of various ratios of KCl and Phosphoric acid were prepared and PABA was dispersed in these solutions. As there are no proper methods to measure or detect the degree of exchange, the resistance values from the sensors prepared using the five different PABA solutions might give an idea of the doping levels. The resistance value of the sensors prepared from these five

solutions were measured. The baseline resistance value increases due to the influence of KCl ions on PABA. Though the baseline resistance value increases (Table 5.2), the detection range of the sensor remains the same and the saturation effect is observed above 2455 ppm levels (Figure 5.16).

The sensitivity of sensor's performance is also dependent on the surface-to-volume ratio of the polymer material.

Table 5.2 Variation in resistance due to change in ratio of H_3PO_4 and KCl suspension solutions used for synthesizing PABA.

Solutions	Concentrations of Solutions Used for Suspending Synthesized PABA	Baseline Resistance in Air (Ohms) - PABA only No Nafion	Baseline Resistance in Air (Ohms) – PABA and Nafion
s1	0.1 M H_3PO_4 (100 ml)	3840	16,772
s2	70 ml of 0.1 M H_3PO_4 + 30 ml of 0.1 M Kcl	7360	64,108
s3	50 ml of 0.1 M Kcl + 50 ml of 0.1 M H_3PO_4	5006	90,274
s4	30 ml of 0.1 M H_3PO_4 + 70 ml of 0.1 M Kcl	6385	304,548
s5	100 ml of 0.1 M Kcl	8158	191,700

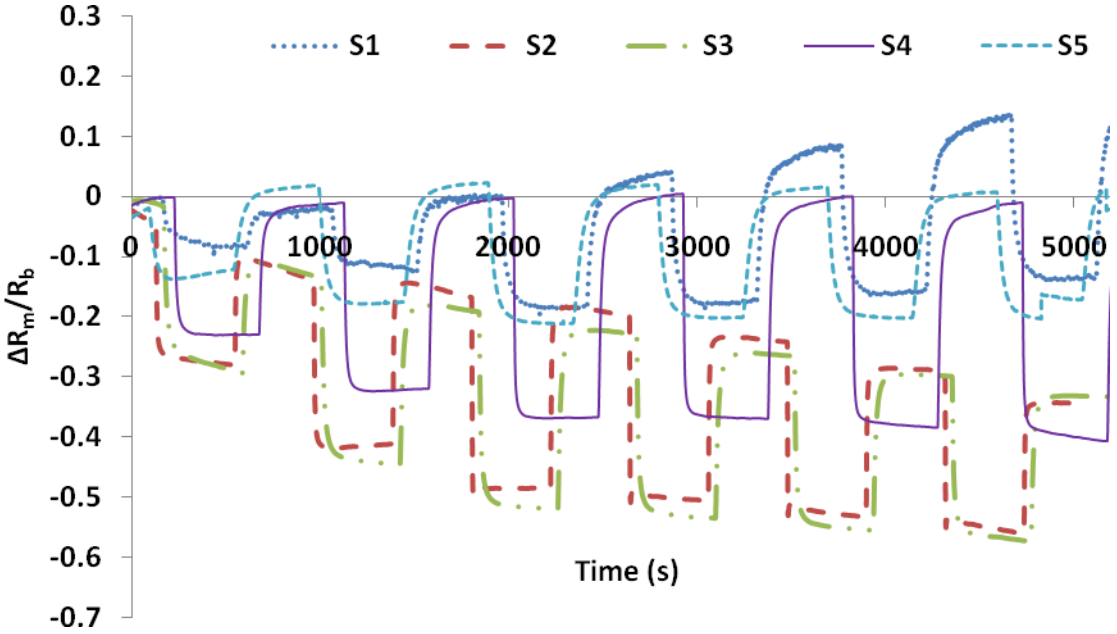

(a)

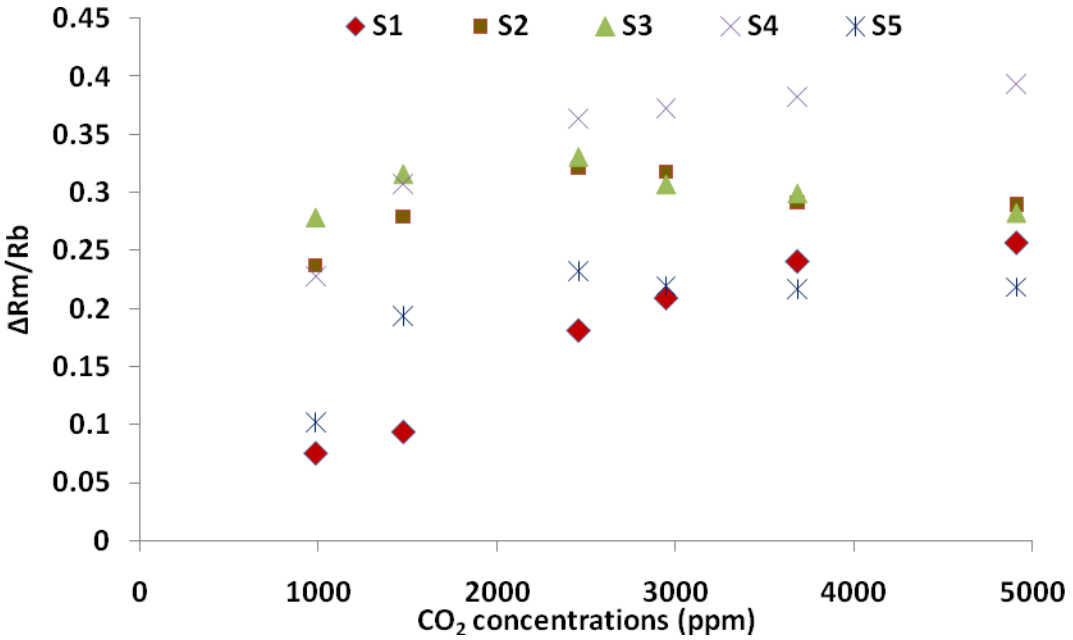

(b)

Figure 5.16 (a), (b) Response of PABA Nafion sensor prepared with 5 different solutions to various concentrations of CO_2 at 50% RH and at 25°C.

5.12 Sensor Packaging

Miniature sensor elements will usually not function on their own. The sensor packaging gives the sensor a suitable shape or form, provides electrical connection to the sensor, and provides a window from the sensor to the outside world. In addition, the sensor elements need mechanical and chemical protection. To package the CO_2 sensor for preliminary testing in bulk grain several options were considered to ensure that the packaging components avoid contamination of the sensing material and the substrate by undesirable components including grain dust and foreign material in grain. The dimensional details of the sensor chip and gas diffusion properties of the packaging material were considered in selecting the packaging components. The performance characteristics of the sensors depend on the geometry of electrodes, thermal design of the structure and the nature of the electronic interface. On practical applications, there will be a trade off between cost and performance.

5.13 Grain Bulk Measurement

The CO_2 sensor packaged in the prototype housing assembly (Figure 5.17) was tested in plastic pails (4 L capacity) filled with wheat. The pails were purged with different CO_2 concentrations to simulate spoilage of grain. The sensor exhibited excellent response (Fig 5.18) to change in CO_2 levels inside grain bulk. The CO_2 gas at desired levels was passed through the bottom of the pail while the sensor was kept immersed in the grain bulk at the top. The plastic pail was

covered tightly with duct tape to prevent atmospheric exchange into the grain bulk. Gas samples from the outlet tube were analyzed using GC-MS to determine the concentrations of the outlet gas.

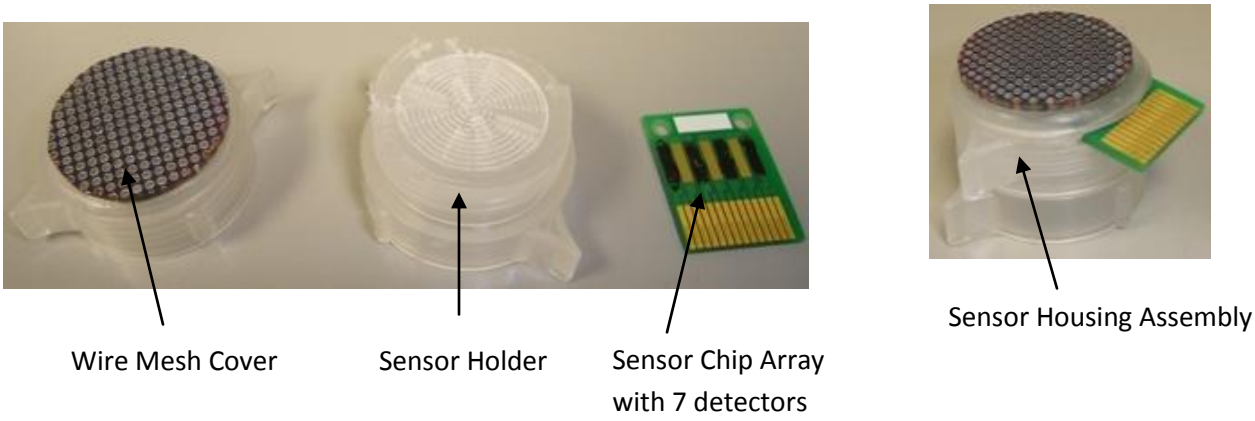

Figure 5.17 Picture of the Sensor Housing Assembly Packaging

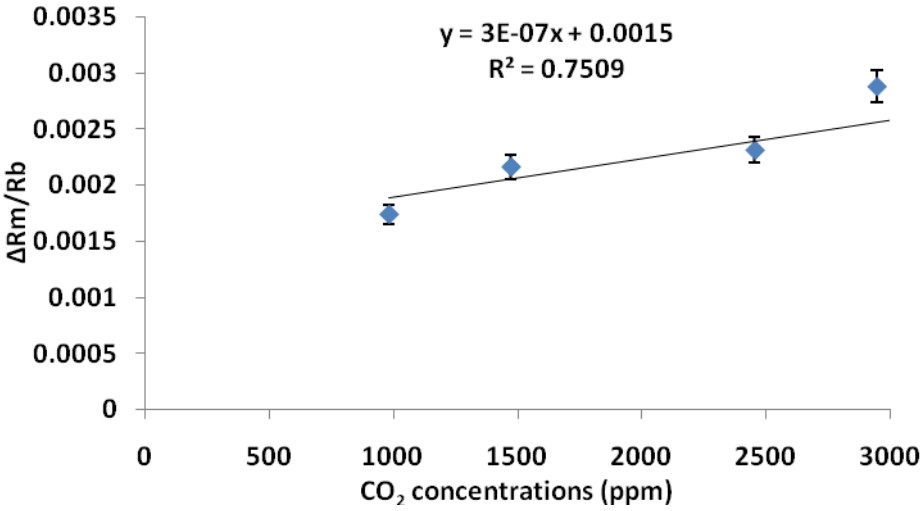

Figure 5.18 Response of PABA Nafion Sensor with packaging kept inside grain bulk to concentrations of CO_2 at 50% RH and at 25°C for 5 replicates.

6. CONCLUSIONS

The co-occurrence of insect and fungal species inside bulk wheat produced new volatile metabolites. Methyl isobutyl ketone is a new compound identified in this study as a result of co-occurrence of multiple species inside the wheat bulk. The results of this research provide information that can be used in the development of odour sensor arrays. More knowledge is necessary to understand the patterns of interrelations among insects and fungi within wheat bulks for quantification of the volatile concentrations.

A sensitive tool for detecting incipient or ongoing deterioration of stored grains by measuring CO_2 levels was developed using PABA conducting polymer. The CO_2 sensor can monitor the CO_2 concentration, which requires water in the air to operate, permitting the detection of CO_2 between 20 to 70% equilibrium relative humidity. The sensor dynamically detected up to 2455 ppm of CO_2 levels in the grain bulk. The CO_2 sensor exhibited dynamic performance in its response, recovery time, sensitivity, selectivity, stability and response slope. The CO_2 sensor responded well to various concentrations of CO_2 at temperatures between 25°C to 55°C. The sensors respond to various levels of CO_2 at ambient temperature without artificial cooling. The packaging unit allowed measurement of CO_2 concentration in grain bulk. The methodology used for building the CO_2 sensor device is compatible with the MEMS process (printed circuit board process) and can be mass manufactured using screen printing technology.

7. REFERENCES

Barsan, N. and U. Weimar. 2001. Conduction of model of metal oxide gas sensors. *Journal of Electroceramics*, 7: 143–167.

BCC Research. 2003. Gas sensors and gas metering: applications and markets. Norwalk, CT, USA. BCC Corporation Company.

Bultzingslowen, C.V., A.K. McEvoy, C. McDonagh, B.D. MacCraith, I.M. Klimant and C.Krausec. 2002. Sol–gel based optical carbon dioxide sensor employing dual luminopore referencing for application in food packaging technology. *Analyst* 27:1478–83.

Capone, S., A. Forleo, R. Francioso, P. Rella, J. Spadavecchia, S. Presicce and A.M. Taurino. 2003. Solid state gas sensors: state of the art and future activities. *Journal of Optoelecronics and Advanced materials* 5(5): 1335-1348.

Cattrall, R.W. 1997. *Chemical sensors*. Oxford, UK. Oxford University Press.

Chittester, C. 1996. An analysis of chemical and biological parameters of an isolated fresh-water environment. http://www.utc.edu/Faculty/Gary-Litchford/Main/report.html (2008/05/06).

Colin, F., T.J.N. Carter and J.D. Wright. 2003. Modification of a piezo-optical gas dosimeter system towards continuous gas sensing: a feasibility study with carbon dioxide. *Sensors and Actuators B*. 90: 216–21.

Coppock, R. 1998. Implementing the Kyoto Protocol. Issues in Science and Technology, Washington, DC. National Academy of Sciences.

CTEH. 2007. TO-14 Analytes using a portable GC/MS. Application Note, Center for Toxicology and Environmental Health, University of Arkansas, Fayetteville, AR.

Cui, G., J.S. Lee, S.J. Kim, H. Nama, G.S. Cha and H.D. Kim. 1998. Potentiometric pCO_2 sensor using polyaniline-coated pH-sensitive electrodes. *Analyst* 123: 1855–1859.

Datta, A.K. 1992. Sensors and food processing operations. In *Encyclopedia of Food Science and Technology,* ed. Y.H. Hui, 2327-2333. New York, NY: John Wiley and Sons.

Dean, J.A. 1998. *Lange's Handbook of Chemistry*, 15th edition. New York, NY: McGraw Hill.

Deore, B.A., S. Hachey and M.S. Freund. 2004. Electroactivity of

electrochemically synthesized Poly(Aniline Boronic Acid) as a function of pH: role of self doping. *Chemistry of Materials*, 16: 1427–1432.

Deore, B.A., M.D. Braun and M.S. Freund. 2006. pH dependent equilibria of

poly(anilineboronic acid)-saccharide complexation in thin films. *Macromolecular Chemistry and Physics* 207: 660-664.

Deore, B.A. and M.S. Freund. 2009. Self doped polyaniline nanoparticle

dispersions based on boronic acid-phosphate complexation. *Macromolecules* 42: 164-168.

Diagne, E.H.A and M. Lumbreras. 2001. Elaboration and characterization of tin oxide–lanthanum oxide mixed layers prepared by the electrostatic spray pyrolysis technique. *Sensors and Actuators B* 78: 98–105.

Dickinson, T.A., J. White, J.S. Kauer and D.R. Walt. 1998. Current trends in artificial nose technology. *Trends in Biotechnology 1*6(6): 250–258.

Dieckmann, M. and R. Buchholz. 1999. Apparatus for measuring the partial pressure of gases dissolved in liquids. *US Patent 6003362.*

English, J.T., B.A. Deore, and M.S. Freund. 2006. Biogenic amine vapor detection using poly(anilineboronic acid) films, *Sensors and Actuators B*, 115: 666-671.

Fabre, B. and L. Taillebois. 2003. Poly(aniline boronic acid)-based conductimetric sensor of dopamine. *Chemical Communications*, 24: 2982-2983.

FAO. 2000. Crop and food supply assessment. FAO Corporate Document Depository: Economic and Social Department, United Nations, Rome, Italy.

Fernando, W.G.D., R. Ramarathnam, A.S. Krishnamoorthy and S.C. Savchuk. 2005. Identification and use of potential bacterial organic antifungal volatiles in biocontrol. *Soil Biology and Biochemistry* 37(5): 955-964.

Freund, M.S. and Deore, B. 2007. Self-doped conducting polymers, 1st edition. Chicester, England: John Wiley and Sons.

Frost and Sullivan. 2000. *World flow sensor markets*. Report 7261-32. London, UK. Frost and Sullivan Consulting Company.

Greenspan, L. 1977. Humidity fixed points of binary saturated aqueous salt solutions. *Journal of the Research National Bureau of Standards-A, Physics and Chemistry* 81(1): 89-96.

Haeusler, A. and J. Meyer. 1996. A novel thick film conductive type carbon dioxide sensor. *Sensors and Actuators B* 34(1-3): 388–395.

Herber, S., J. Bomer, W. Olthuis, P. Bergveld and A.V. Berg. 2005. A miniaturized carbon dioxide gas sensor based on sensing of pH-sensitive hydrogel swelling with a pressure sensor. *Biomedical Microdevices* 7(3): 197–204.

Hooker, S.A. 2002. Nanotechnology advantages applied to gas sensor development. *The Nanoparticles 2002 Conference Proceedings,* Norwalk, CT: Business Communications Company Inc.

Hu, I., B. Vincenzo, T. Vincenzo, A. Antonino and A. Vincenzo. 2008. PEO-PPO-PEO triblock copolymer/Nafion blend as membrane material for intermediate temperature. *DMFCs Journal of Applied Electrochemistry* 38(4): 543-550.

Ileleji, K.E., D.E. Maier, C. Bhat and C.P. Woloshuk. 2006. Detection of a developing hot spot in stored corn with a CO_2 sensor. *Applied Engineering in Agriculture* 22: 275-289.

Irimia-Vladu, M. and J.W. Fergus. 2006. Suitability of emeraldine base polyaniline-PVA composite film for carbon dioxide sensing. *Synthetic Metals* 156: 1401–1407.

Ishihara, T., K. Kometani, M. Hashida and Y. Takita. 1991. Application of mixed oxide capacitor to the selective carbon dioxide sensor. *Journal of Electrochemical Society* 138(1): 173–176.

Jasinski, G., P. Jasinski, B. Chachulski and A. Nowakowski. 2006. Electrocatalytic gas sensors based on Nasicon and Lisicon. *Materials Science* 24(1): 261-267.

Jayas, D.S. 1995. Mathematical modeling of heat, moisture, and gas transfer in stored-grain ecosystems. In *Stored Grain Ecosystems*, 527-567. New York, NY: Marcel Dekker Inc.

Jayas, D.S., D.A. Irvine, G. Mazza and S. Jeyamkondan. 2001. Evaluation of a computer-controlled ventilation system for a potato storage facility. *Canadian Biosystems Engineering* 43(5): 5–12.

Jensen, M.A. and G.A. Rechnitz. 1979. Response time characteristics of the pCO2 electrode. *Analytical Chemistry* 51(12): 1972-1977.

Jones, C.L. 1923. The uses of carbon dioxide-I. *Canadian Chemistry and Metallurgy* 7(7): 172-174.

Kaneyasu, K, K. Otsuka, Y. Setoguchi, S. Sonoda, T. Nakahara and I. Aso. 2000. A carbon dioxide gas sensor based on solid electrolyte for air quality control. *Sensors and Actuators B* 66: 102–106.

Karasek, F.W. and R.E. Clement. 1988. *Basic Gas Chromatography - Mass Spectrometry: Principles and Techniques*, 1st edition. Amsterdam, The Netherlands: Elsevier Science Co.

Kim, D., J. Yoon, H. Park and K. Kim. 2000. CO_2 sensing of SnO_2 thick film by coating lanthanum oxide. *Sensors and Actuators B* 62(1): 61–66.

Kinkade, B.R. 2000. Bringing nondispersive IR spectroscopic gas sensors to the mass market. *Sensors Magazine* 9: 83.

Lees M. 2003. *Food Authenticity and Traceability*. Cambridge, UK. Wood Head Publications.

Lee, D., S. Choi and K. Lee. 1995. Carbon dioxide sensor using NASICON prepared by the sol-gel method. *Sensors and Actuators B* 24: 607–609.

Lee, D and D. Lee. 2001. Environmental gas sensors. *IEEE Sensors Journal* 1(3): 214–224.

Li, G., M. Josowics, J. Janata and S. Semancik. 2004. Effect of thermal excitation on intermolecular charge transfer efficiency in conducting polyaniline *Applied Physics Letters* 85(7): 1187-1189.

Loschiavo, S.R., J. Wong, N.D.G. White, H.D. Pierce, J.H. Borden and A.C. Oehlschlager. 1986. Field evaluation of a pheromone to detect adult rusty grain beetles, *Cryptolestes ferrugineus* (Coleoptera: Cucujidae), in stored grain. *The Canadian Entomologist* 118: 1-8.

Madrid, F.J., N.D.G. White and S.R. Loschiavo. 1990. Insects in stored cereals and their association with farming practices in southern Manitoba. *The Canadian Entomologist* 122: 515-523.

Magan, N. and P. Evans.2000. Volatiles and indicators of fungal activity and differentiation between species, and the potential use of electronic nose technology for early detection of grain spoilage. *Journal of Stored Products Research* 36: 319-340.

Mahmoudi, B, N. Gabouze, L. Guerbous, M. Haddadi, H. Cheraga and K. Beldjilali. 2007. Photoluminescence response of gas sensor based on CHx/porous silicon – effect of annealing treatment. *Materials Science and Engineering B* 138(3): 293–297.

Maier, D., R. Hulasare, B. Qian and P. Armstrong. 2006. Monitoring carbon dioxide levels for early detection of spoilage and pests in stored grain. *Proceedings of the 9th International Working Conference on Stored Product Protection,* October 15-18. Sao Paulo. Brazil.

Mandayo, G.G, F. Gonzalez, I. Rivas, I. Averdi and J. Herran. 2006. BaTiO3–CuO sputtered thin film for carbon dioxide detection. *Sensors and Actuators B* 118(1- 2): 305–310.

Marazuela, M.D., M. Bondi, C. Maria and G. Orellana. 1998. Luminescence lifetime quenching of a ruthenium (II) polypyridyl dye for optical sensing of carbon dioxide. *Applied Spectroscopy* 51(10): 1257-1367.

MNT. 2006. Microtechnology nano network gas sensor road map. London, UK: The Council of Gas Detection and Environment Monitoring.

Moseley, P.T. 1997. Solid state gas sensors. *Measurement Science and Technology* 8: 223–237.

Muir, W.E., D. Waterer and R.N. Sinha. 1985. Carbon dioxide as an early indicator of stored cereal and oilseed spoilage. *Transactions of the ASAE* 28: 1673–1675.

Mulrooney, J., J. Clifford, C. Fitzpatrick and E. Lewis. 2006. Detection of carbon dioxide emissions from a diesel engine using a mid-infrared optical fibre based sensor. *Sensors and Actuators A* 136: 104–110.

Muller, B. and P.C. Hauser. 1996. Fluorescence optical sensor for low concentrations of dissolved carbon dioxide. *Analyst* 121 (3): 339–343.

Nagel, D.J. and S. Smith. 2003. Nanotechnology enabled sensors: possibilities, realities and applications. http://www.sensormag.com/sensors/articledetail. Jsp?id =361237 (2008/06/11).

Nakamura, N. and Y. Amao. 2003. An optical sensor for CO_2 using thymol blue and europium (III) complex composite film. *Sensors and Actuators B* 82: 98–101.

Neethirajan, S., D.S. Jayas and S. Sadistap. (2009) Carbon dioxide (CO2) sensors for the agri-food industry - A Review. *Food and Bioprocess Technology* 2(2): 115-121.

Ogura, K., and H. Shiigi. 1999. A CO_2 sensing composite film consisting of base type polyaniline and poly(vinyl alcohol). *Electrochemical and Solid-State Letters* 2(9): 478-480.

Oho, T., T. Tonosaki, K. Isomura and K. Ogura. 2002. A CO_2 sensor operating under high humidity. *Synthetic Metals* 522: 173–178.

Parvatikar, N., S. Jain, S. Khasim, M. Revansiddappa, S.V. Bhoraskar, M.V.N.A, Prasad. 2006. Electrical and humidity sensing properties of polyaniline/WO3 composites. *Sensors and Actuators B* 114: 599-603.

Pasierb, P., S. Komornicki, S. Kozinski, R. Gajerski and M. Rekas. 2004. Long-term stability of potentiometric CO_2 sensors based on Nasicon as a solid electrolyte. *Sensors and Actuators B* 101: 47–56.

Prokes, J. and J. Stejskal. 2004. Polyaniline prepared in the presence of various

acids 2.Thermal stability of conductivity. *Polymer Degradation and Stability* 86: 187-195.

Rego, R. and A. Mendes. 2004. Carbon dioxide/methane gas sensor based on the permselectivity of polymeric membranes for biogas monitoring. *Sensors and Actuators B* 103: 2–6.

Reich, G.T. 1945. Carbon dioxide in the food industry. *Food Industries* 17(11): 93-95.

Schaller, E., J.O. Bosset and F. Escher. 1998. Electronic noses and their application to food. *Lebensmittel-Wissenschaft und-Technologie* 31(4): 305-316.

Segawa, H., E. Ohnishi, Y. Arai and K. Yoshida. 2003. Sensitivity of fiber-optic carbon dioxide sensors utilizing indicator dye. *Sensors and Actuators B* 94: 276–281.

Seitz, L.M. and M.S. Ram. 2000. Volatile methoxybenzene compounds in grains with off-odours. *Journal of Agricultural Food Chemistry* 48: 4279-4289.

Semple, R.L., P.A. Hicks, V. Lozare and A. Castermans. 1988. Towards integrated commodity and pest management in grain storage, Proceedings of the Integrated Pest Management Strategies in Grain Storage Systems Conference, National Post Harvest Institute for Research and Extension (NAPHIRE), Department of Agriculture, June 6-18, Philippines.

Severinghaus, J.W and A.F. Bradley. 1958. Electrodes for blood pO_2 and pCO_2 determination. *Journal of Applied Physiology* 13: 515–520.

Shimizu Y. and N. Yamashita. 2000. Solid electrolyte CO_2 sensor using NASICON and Perovskite type oxide electrode. *Sensors and Actuators B* 64: 102–106.

Shoji, E. and M.S. Freund. 2002. Potentiometric saccharide detection based on the pKa changes of poly(aniline boronic acid). *Journal of American Chemical Society* 124: 12486-12493.

Singh (Jayas), D., W.E. Muir and R.N. Sinha. 1983. Finite element modelling of carbon dioxide diffusion in stored wheat. *Canadian Agricultural Engineering* 25: 149–152.

Sinha, R.N., D. Tuma, D. Abramson and W.E. Muir. 1988. Fungal volatiles associated with mouldy grain in ventilated and non ventilated bin-stored wheat. *Mycopathologia* 101: 53-60.

Sipior, J., L. Randers-Eichhorn, J.R. Lakowics, C.M. Carter and G. Rao. 1996. Phase fluormetric optical carbon dioxide gas sensor for fermentation off-gas monitoring. *Biotechnology Progress* 12: 266–271.

Skoog, D.A. 1985. *Principles of Instrumental Analysis,* 5th edition. Philadelphia, PA: Saunders Book Company.

Skotheim, T.A., R.L. Elsenbaumer and J.R. Reynolds. 1998. Handbook of conducting polymers. Boca Raton, FL: CRC Press.

Smith, R.L. 1996. Ecology and field biology, 5th edition. New York, NY: Harper Collins College Publishers.

Smolander, M., E. Hurme and R. Ahvenainen. 1997. Leak indicators for modified-atmosphere packages. *Trends in Food Science and Technology* 8: 101–106.

Solomon, M.E. 1951. Control of humidity with potassium hydroxide, sulphuric acid, or other solutions. *Bulletin of Entomological Research* 42: 543-554.

Statistics Canada, 2007. Canadian Exports and Imports. http://www.statcan.ca/english/freepub/15-515-XIE/2004001/export.htm#3 (2007/03/20).

Stumm, W. and J.J. Morgan. 1995. Aquatic Chemistry - Chemical Equilibria and Rates in Natural Waters, 3rd edition. New York, NY: Wiley Intersciences Publishers.

Suzuki, H., T. Hirakawaa, S. Sasakib and I. Karubeb. 2000. An integrated module for sensing pO_2, pCO_2, and pH. Analytica Chimica Acta 405(1-2): 57-65.

Takeda, S. 1999. A new type of CO_2 sensor built up with plasma polymerized poly aniline thin film. *Thin Solid Films* 343: 313–336.

Tan, E.S., D.C. Slaughter and J.F. Thompson. 2005. Freeze damage detection in

oranges using gas sensors. *Post Harvest Biology and Technology* 35: 177-182.

Tongol, B.J., C.A. Binag and F.B. Sevilla. 2003. Surface and electrochemical studies of carbon dioxide probe based on conducting polypyrrole. *Sensors and Actuators B* 93(1-3): 187–196.

USDA. 1996. Using sensors to detect potentially hazardous atmospheres in production agriculture. Baltimore, MD: United States Department of Agriculture.

USDA, 2007. Foreign Agricultural Service Report. World Agricultural Production Circular Series WAP 04-07. Baltimore, MD: United States Department of Agriculture.

Virji, S., J. Huang, R.B. Kaner and B.H. Weiller. 2004. Polyaniline nanofiber gas sensors: Examination of response mechanisms. *Nanoletters* 4: 491-496.

Viswanathan, B. and M. Helen. Is Nafion the Only Choice? *Bulletin of the Catalysis Society of India* 6: 50-66.

Waghuley, S.A., S.M. Yenorkara, S.S. Yawalea and S.P. Yawalea. 2008. Application of chemically synthesized conducting polymer-polypyrrole as a carbon dioxide gas sensor. Sensors and Actuators B: Chemical 128(2): 366-373.

Wallace, H.A.H. and R.N. Sinha. 1981. Causal factors operative in distributional patterns and abundance of fungi: A multivariate study. In *The Fungal Community– its Organisation and Role in Ecosystems*, 233-247. New York, NY: Marcel Dekker Inc.

Wang, L. and R.V. Kumar. 2003. A novel carbon dioxide gas sensor based on solid bielectrolyte. *Sensors and Actuators B*, 88: 292–299.

Ward, B.J., C.C. Liu and G.W. Hunter. 2003. Novel processing of NASICON and sodium carbonate/ barium carbonate thin and thick films for a CO_2 microsensor. *Journal of Material Science* 38: 4289–42992.

Warren, L.F., J.A. Walker, D.P. Anderson, C.G. Rhodes and L.J. Buckley. 1989.

A study of conducting polymer morphology. *Journal of the Electrochemical Society* 136: 2286-2295.

White, N.D.G. 1995. Insects, mites, and insecticides in stored-grain ecosystems. In *Stored Grain Ecosystems*, eds. D.S. Jayas, N.D.G. White and W.E. Muir, 1-32. New York, NY: Marcel Dekker Inc.

Williams, D.E. and K.F.E. Pratt. 2000. Microstructure effects on the response of gas-sensitive resistors based on semiconducting oxides. *Sensors and Actuators B* 70: 214–221.

Yang, Y. and C. Liu. 2000. Development of a NASICON based amperometric carbon dioxide sensor. *Sensors and Actuators B* 62: 30–34.

Zhu, Q, F. Qiu, Y. Quan, Y. Sun, S. Liu and S. Zou. 2005. Solid-electrolyte NASICON thick film CO_2 sensor prepared on small-volume ceramic tube substrate. *Materials Chemistry and Physics* 91: 338–342.